



Development Upgrades of the Atacama Large
Millimeter/submillimeter Array (ALMA)

Final Report

PROTOTYPE OF A COMPLETE DUAL-LINEAR 2SB BLOCK

AND

A SINGLE-POLARIZATION BALANCED 2SB BLOCK

PRINCIPAL INVESTIGATOR: DOUG HENKE

INSTITUTION: NRC HERZBERG ASTRONOMY AND ASTROPHYSICS

ADDRESS: 5071 WEST SAANICH RD, VICTORIA, CANADA

PI CONTACT INFORMATION:

Telephone Number 1-250-363-6937

Email Address Doug.Henke@nrc-cnrc.gc.ca

DATE: OCTOBER 12, 2018

ABSTRACT

During Oct./2016–Sept./2018, the Cycle 4 ALMA Development study, “Prototype of a complete dual-linear 2SB block and a single-polarization balanced 2SB block,” was completed.

Using an existing ALMA B3 cartridge, the receiver front-end was reconfigured into two different receiver architectures:

- DL-2SB: dual-linear sideband-separating
- BAL-2SB: (single-polarization) balanced sideband-separating

The motivation behind the study was to look at ways to increase the packing density of feeds for multi-beam arrays by: (1) using hole couplers to facilitate LO distribution and (2) integrating the OMT with the power divider for 2SB receivers. In addition, a balanced 2SB architecture was implemented to evaluate the possible improvements for Band 3.

Using a platelet configuration, it was shown that hole couplers could be integrated to realize very low values of coupling, while still maintaining machinability and broadband isolation. Since very little of the LO power was lost through each coupler, the LO signal was routed to the next mixer pair so that all four mixers were pumped using the same input. Measurements indicated even pumping and similar performance between mixer pairs, which demonstrated that this approach could be successfully extended for LO distribution within larger detector arrays.

It was also shown that using the turnstile as both a power splitter and OMT did not work well. We did see a drop in the noise (due to lower LO coupling and no image termination), but this was offset by excess ripple in the noise, as well as a degradation in the sideband-separated response.

In the final section of the report, a modified design is shown to make use of the successful LO distribution without integrating the OMT.

CONTENTS

1	INTRODUCTION	1
1.1	Co-Investigators.....	1
1.2	Review of Tasks and Timeline.....	1
1.3	Budget and Study Value	2
2	DL-2SB: DUAL-LINEAR SIDEBAND-SEPARATING	3
2.1	Design Concept and Implementation	3
2.2	Measurements of the DL-2SB Block.....	5
2.3	Cartridge Integration.....	9
3	BAL-2SB	14
3.1	Design Overview	14
3.2	Measurements of the BAL-2SB Block.....	16
3.3	Cartridge Integration.....	18
3.4	A Closer Look at the Turnstile.....	22
4	SUPPLEMENTARY EXPERIMENTS	24
4.1	BAL-DSB: Removing the 90° IF Hybrid.....	24
4.2	Reversing LO/RF Inputs on the B3 Cartridge	25
5	CONCLUSION AND FUTURE OUTLOOK	28
	ACKNOWLEDGMENTS	29
	APPENDIX A - REFERENCE DOCUMENTS	29

1 Introduction

This is the final report on the Cycle 4 Development Study entitled, “Prototype of a complete dual-linear 2SB block and a single-polarization balanced 2SB block” [1]. The full study period extended from Oct./2016 – Sept./2018. An interim report [2] was also delivered and applicable content is repeated here.

1.1 Co-Investigators

Table 1.0: Co-Investigator(s) and Collaborating Institution(s).

NAME	INSTITUTION	EMAIL	TELEPHONE
Doug Henke	NRC Herzberg Astronomy and Astrophysics	Doug.Henke@nrc-cnrc.gc.ca	250-363-6937
Pat Niranjana	NRC Herzberg Astronomy and Astrophysics	Pat.Niranjana@nrc-cnrc.gc.ca	250-363-3255
Lewis Knee	NRC Herzberg Astronomy and Astrophysics	Lewis.Knee@nrc-cnrc.gc.ca	250-363-3075

1.2 Review of Tasks and Timeline

TABLE 1
ORIGINAL SCHEDULE PROPOSED IN [1].

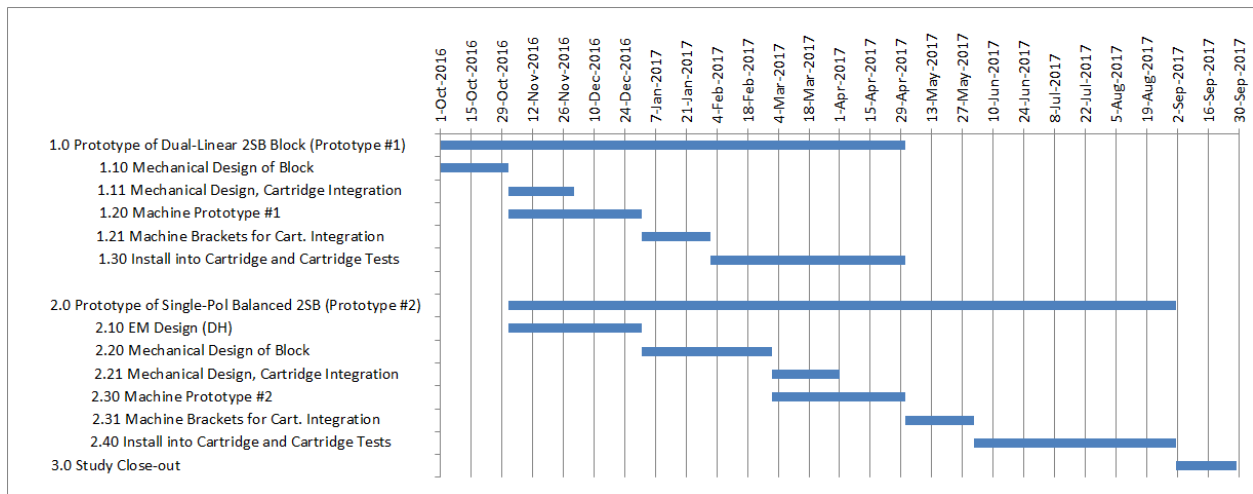


Table 1 shows the original schedule and work-breakdown structure. The proposal was divided into two prototypes: (1) a dual-linear 2SB block (DL-2SB) and (2) a single-polarization balanced 2SB block (BAL-2SB).

In summary, the study took an extra year to complete due to the following factors:

1. The nature of research with unknown outcomes and iterations of re-design. Initial conceptual designs needed to be reworked for cartridge integration and machinability.
2. Labor commitment. Due to multiple projects for each resource, we were not able to devote as many hours originally envisioned within the original timeline.
3. Unforeseen testing upgrades (not charged to project). One of our test sets was in need of upgrading for more reliable mixer testing. In short, the operating system was changed, requiring new software development, and deficiencies were discovered in the LO system (power level and x6 multiplier purity) and DC readout (Keysight MUX intermittent failure).
4. Additional follow-up testing.

1.3 Budget and Study Value

As outlined in the proposal, the budget was broken into: (1) study cost and (2) in-kind contributions by HAA. The study costs were projected at 60% of labor costs for the machinist/technologists supporting the project. In-kind contributions were the remaining labor costs for machinist/technologists and PI labor, facilities, and contingency. The total value of the proposal was forecasted at \$391 k, where ~37% was attributed to study costs (\$145.6 k) and ~63% was contributed in-kind (\$245.4 k). As shown in Fig. 4, actual costs of the study were \$145.6 k (NRAO) and \$253.4 k (NRC HAA) in USD.

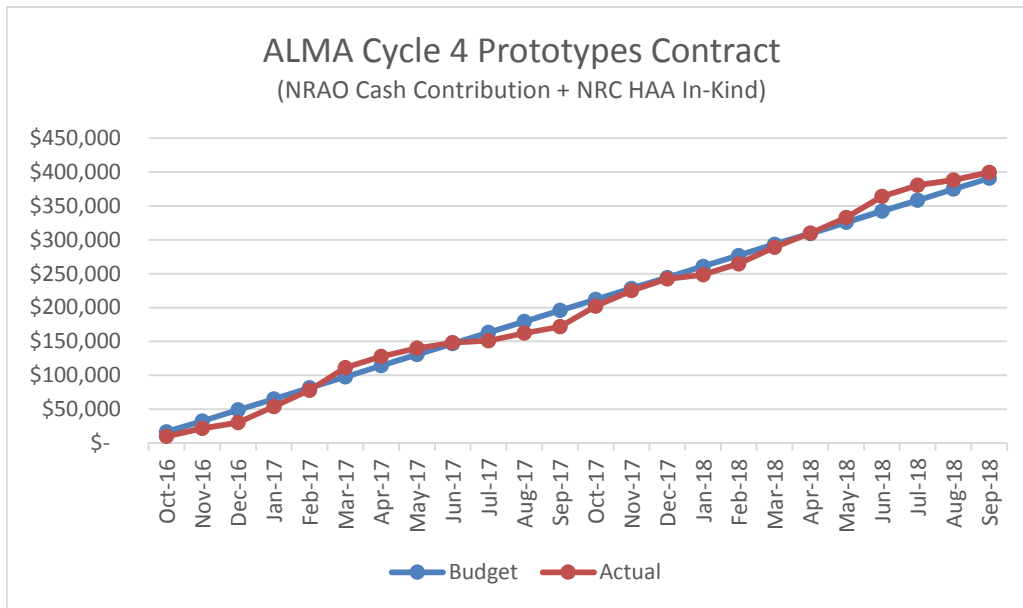


Fig. 1. Actual and forecasted total budget as extended over two years.

2 DL-2SB: Dual-Linear Sideband-Separating

2.1 Design Concept and Implementation

Details on the as-built ALMA Band 3 cartridge can be found in [3] and [4]. The incoming RF signal is separated into two linear polarizations using a Bøfjot OMT, as shown in Fig. 2 and Fig. 3. Each polarized RF signal is then split using a 90° branch-line coupler and the LO is divided using a Y-splitter. After down-conversion, the IF is recombined through a 90° hybrid combiner to achieve sideband-separation.

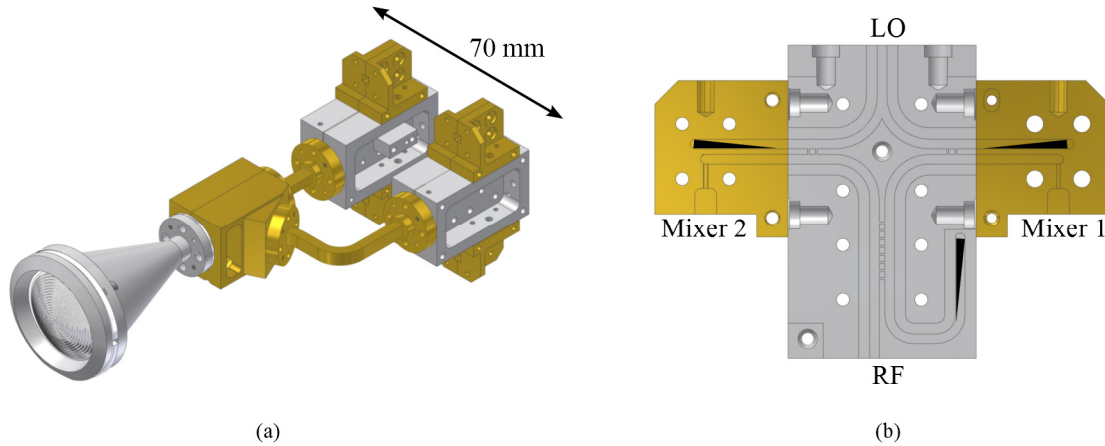


Fig. 2. (a) The dual-linear polarization 2SB assembly as used in the ALMA Band 3 receiver. Separate 2SB blocks are used for each polarization. (b) Open view of the RF/LO waveguide splitter network with mixer blocks (colored grey and gold respectively). The waveguides have been sectioned along the E-plane following a split-block approach.

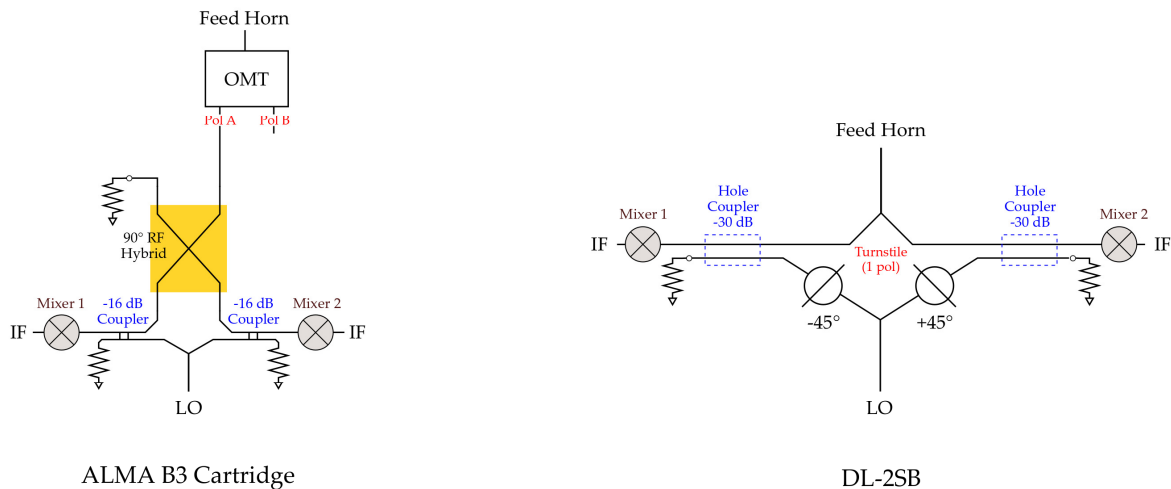


Fig. 3. Block diagram of the ALMA Band 3 cartridge compared against the dual-linear sideband-separating (DL-2SB) block architecture. Only one polarization is shown for clarity.

One of the design goals of this study was to explore the use of a turnstile for both polarization separation and RF power division by integrating the OMT with the 2SB power divider to give a more compact configuration and possibly be used for compact detector arrays.

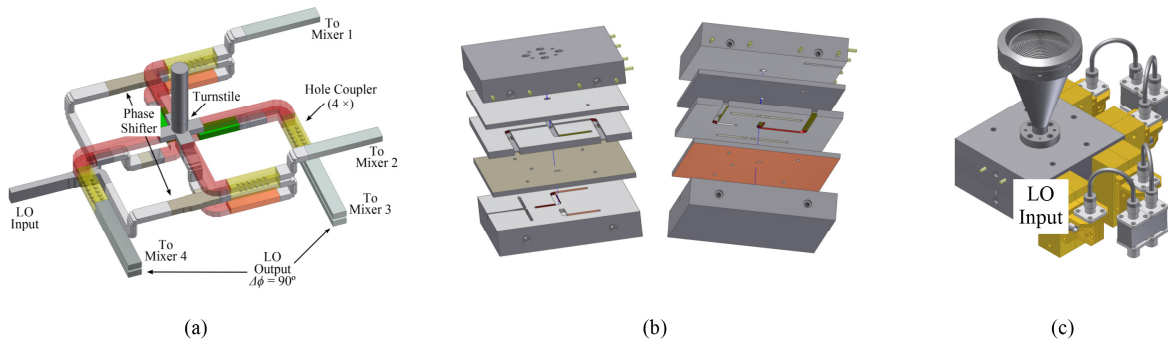


Fig. 4. Originally proposed dual-linear 2SB (DL-2SB) block. The waveguide features are shown in (a) with the block and assembly shown in (b) and (c).

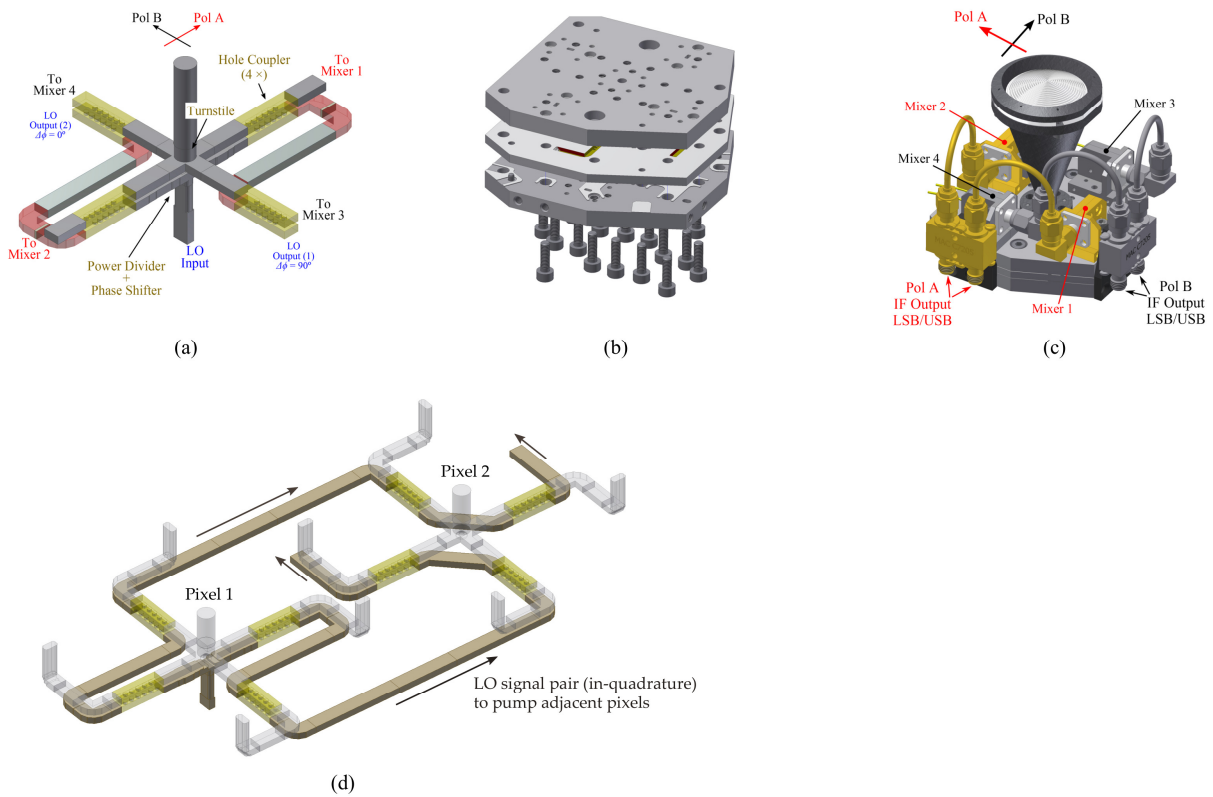


Fig. 5. Realized DL-2SB prototype. The waveguide model is shown in (a) and the resulting 3-piece block and assembly is shown in (b) and (c) respectively. Since the LO coupling is very weak, the LO may continue in its routing to pump additional mixers, as shown in (d).

Fig. 4 and Fig. 5 describe the design flow from concept to the realized DL-2SB prototype. The new model was improved in the following ways:

- Mixer and LO waveguides along same planes
- LO input from bottom for easier integration with cartridge
- Mixer blocks attached from top to fit assembly within cartridge volume
- 3-piece block assembly

In this design, the turnstile performs the polarization separation and power division for sideband-separation. The LO signal is split using a Y-junction and followed by a pair of phase shifters to effect a 90° difference. The phase shifters are similar to [5] except that step impedances are used instead of stubs. Using broad-wall hole couplers, the LO is coupled into the RF signal path: first for mixers 1 & 2, then followed by mixers 3 & 4. Since the amount of LO coupling is very low, approximately -30 dB, the LO signal may be reused to pump the other mixer pair (and possibly more mixers in the case of arrays, as shown in Fig. 5 (d)). An overview of the design is given in [6].

2.2 Measurements of the DL-2SB Block

One of the goals of the proposal was to explore an integrated, platelet-type design that could be suitable for multi-pixel array receivers. This type of design could be stacked to allow for a dense sampling within the focal plane of dual-linear 2SB receivers. As a first step, we wanted to explore the overall machinability of the block, performance of the hole couplers for LO coupling, and the suitability of reusing the LO signal to pump both mixer pairs at once.

The block was machined from AL 6061-T6 and characterized using a vector network analyzer, as shown in Fig. 6; it is an 8-port device with the following port designations:

- Port 1: RF signal input (i.e., through the feed horn) with two linear polarizations
- Ports 2–5: outputs to mixer blocks
- Port 6: LO input
- Ports 7–8: output of LO signal after coupling

Note that ports 7–8 could be internally terminated, but the outputs were kept for measurement validation and to see how suitable the LO output would be to continue pumping even more mixers. A subset of the measurements are shown in Fig. 7 and Fig. 8. A few general comments can be made at the outset. First, measurements agree well with simulated values in CST Microwave Studio, but this comparison is not included for brevity. Second, the bandwidth was widened past the current operating range for both the LO and RF; in retrospect, limiting the bandwidth—especially for the LO path—may be something for future exploration. Third, the power division is achieved by means of a Y-splitter; this is true for both the LO and RF signals (where the turnstile may be considered a Y-splitter for each polarization). Y-splitters are 3-port devices and cannot have all ports simultaneously matched for low power reflection. The design has favored the input (ports 1 and 6) for lowest power reflection.

Fig. 7 shows the balance and impedance match for the RF signal. The turnstile was tuned for very wide input bandwidth, exceeding the current operating bandwidth for Band 3. While the amplitude and phase balance is very good, there are sharp dips in the responses which can most likely be attributed to trapped higher-order modes. Since the measurements at port 1 use a rectangular-to-circular transition (to inject for a given linear polarization), higher order modes of the circular port are shorted and reflected back into the block during the measurement. In Fig. 7 (c), this effect is shown when looking at the mixer port reflection (shown right) and comparing the result between when the circular port was connected through a rectangular transition (solid line) versus when the circular port was terminated using a feed horn (dotted line). Using the turnstile as a power splitter assumes that the circular port will be terminated with a circular termination (i.e., a feed horn is used) and that higher order modes are reflected out this port. Fig. 7 (c) also shows that, in the upper half of the band, the port reflection improves beyond what would be expected of a single-mode 3-port device as there is some mode conversion.

The poor output match at the mixer port is a potential problem for any spurious signals that may be generated within the mixer (e.g., the image spurious response). In this case, the spurious signal that enters the output ports of the DL-2SB will be reflected back into the mixer. Although not shown in Fig. 7 for brevity, the port-to-port mixer isolation is also $\sim 8\text{--}15$ dB.

Simulation has shown that if the output ports are combined, and treated as a balanced pair, the balanced mixers port reflection is quite low. However, this is an ideal case, since mixer reflections within each polarization cannot be guaranteed to be exactly equal in phase and amplitude. Unequal mixer port reflections can leak back into the other mixer of the polarization pair or may also leak into the other polarization. Whether or not the mixers can effectively act together as a balanced pair is the crux of the design. Existing ALMA cartridge designs use a 4-port quadrature hybrid for power division, which have the advantages of impedance matching all 4 ports, terminating reflections, and providing isolation between mixers; the trade-off to the 4th port termination is added noise to the receiver (see [3], [4], [7], and [8] for a comprehensive discussion) which has the most relative impact to Band 3.

Fig. 8 shows the measured responses concerning the LO path. Recall that for an image rejection of 20 dB, the overall amplitude and phase balance should be within 1 dB and 10° . Of first note, the LO coupling to each mixer pair appears to work quite well. Compared to the -16 dB coupling of the existing Band 3 design, the hole coupler provides much lower coupling value while still maintaining machinability. The amplitude and phase balance is similar for both polarizations and is preserved at the output such that, presumably, more mixer pairs could also be pumped, as shown in Fig. 8 (d). As mentioned earlier, the bandwidth far exceeds the required LO tuning range so limiting the bandwidth could improve the LO balance further. In fact, while using a Y-splitter plus combined phase shifter allows for a compact platelet configuration, the phase shifters create ripple in the response because they break perfect symmetry with respect to the turnstile axis. Even still, the LO amplitude and phase balance is approximately 1 dB and 7° and we assume that that this variation in LO pumping between the mixer pairs would still be acceptable in the resulting mixer gain balance.

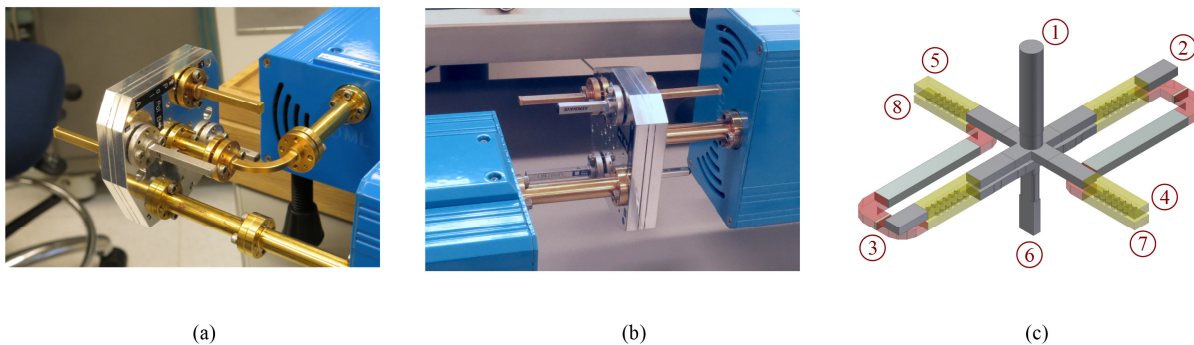


Fig. 6. Examples of vector network analyzer (VNA) measurements for the DL-2SB prototype block. A measurement of the RF signal power division is shown in (a) where port 1 of the VNA is attached to a rectangular-circular transition and port 2 measures the outputs where a mixer block would be attached. In (b), a measurement of the LO-to-mixer coupling is shown where port 2 of the VNA is attached to the LO input and port 1 is connected to the output for one of the mixer blocks. Port designations are shown in (c). Note that this model does not show the final waveguide bends for the output ports.

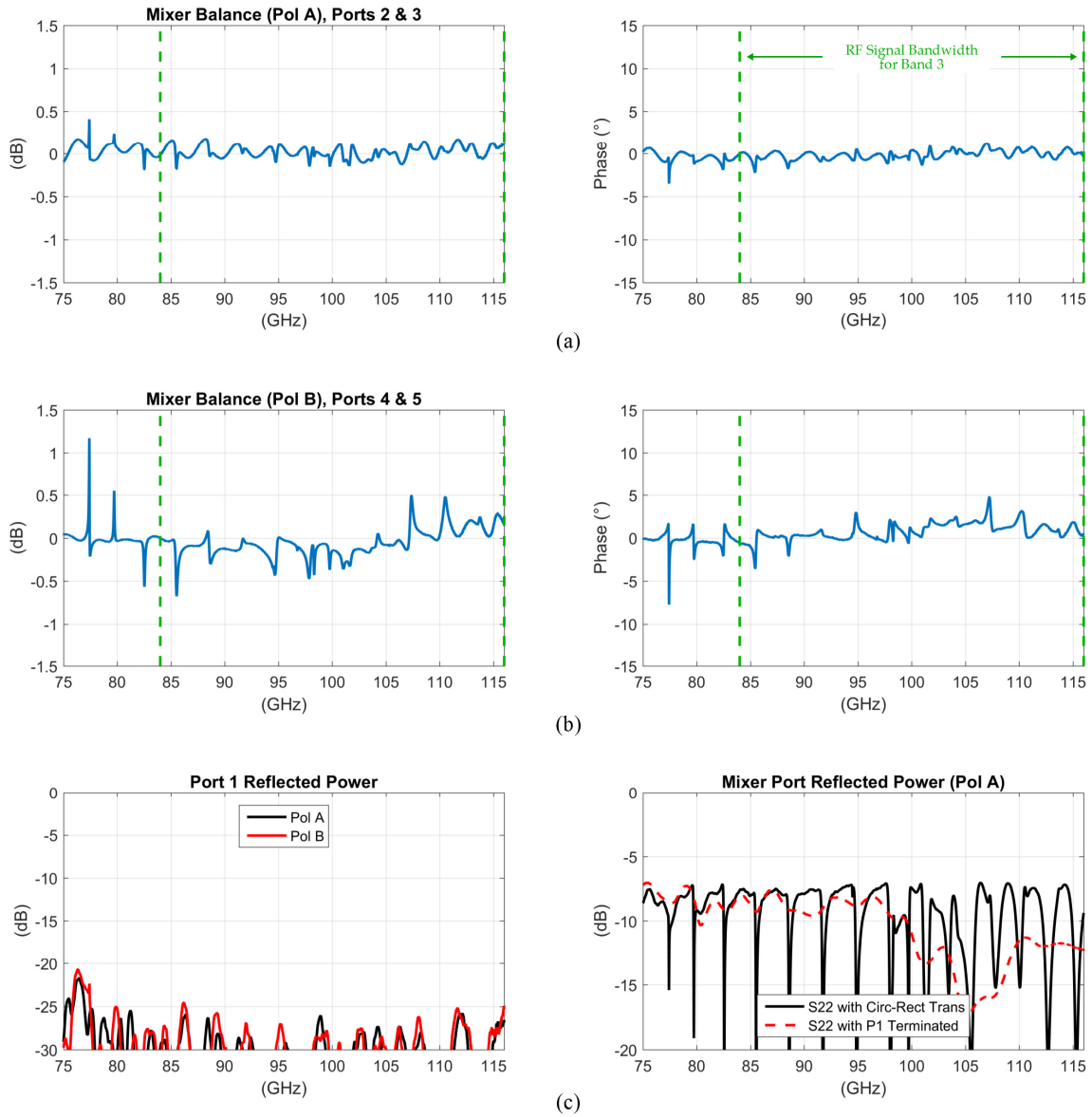


Fig. 7. Room temperature measurements of the RF Signal within the DL-2SB (75–116 GHz with 4001 points). ALMA B3 currently operates between 84–116 GHz. See also Fig. 18.

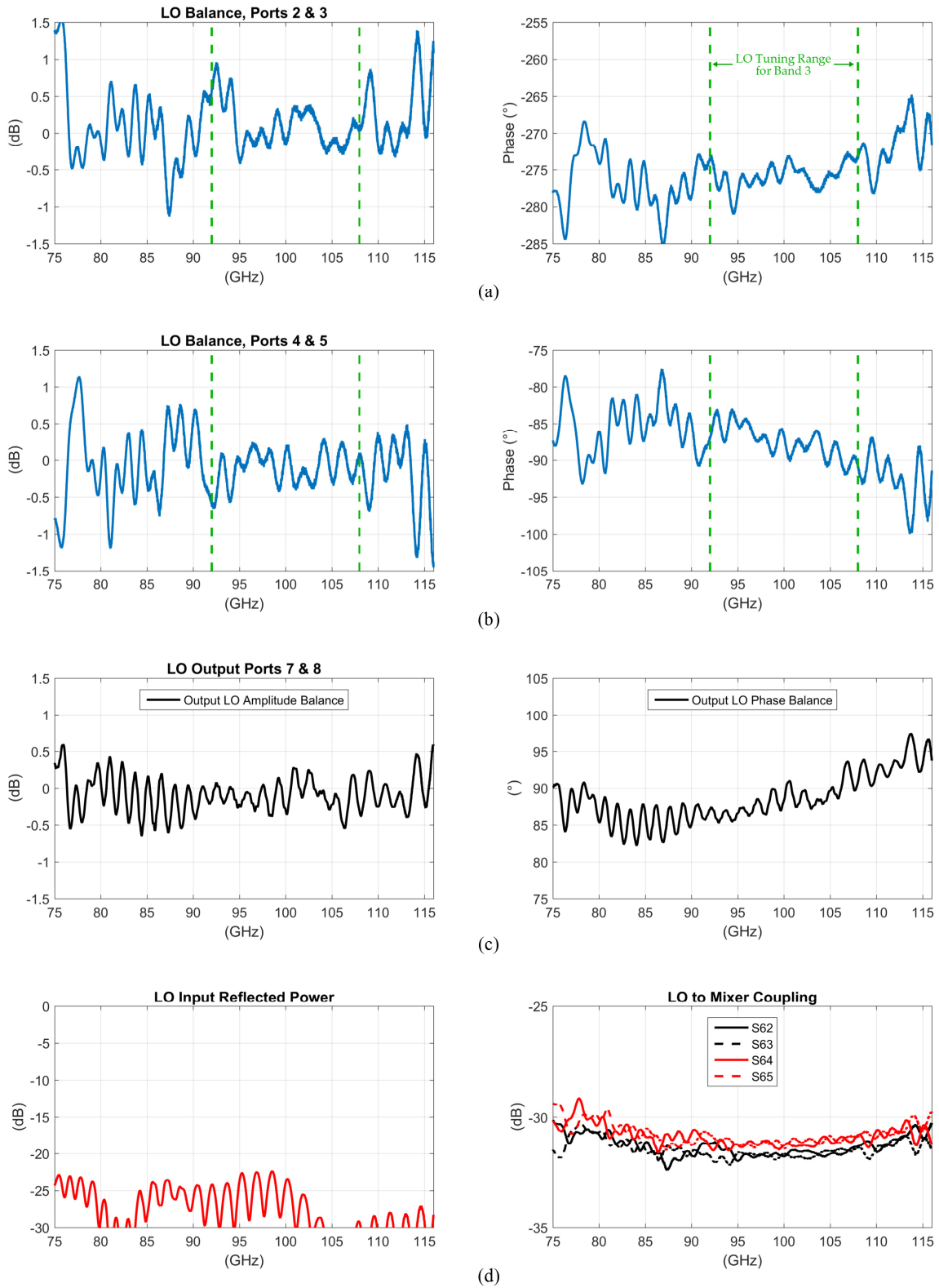


Fig. 8. Room temperature measurements of the LO Signal within the DL-2SB (75–116 GHz with 4001 points). The LO for ALMA B3 currently operates between 92–108 GHz.

2.3 Cartridge Integration

Significant effort went in to integrating the DL-2SB within the B3 cartridge to ensure that everything fit within the allowable volume. This was a necessary step so that careful comparative measurements could be made between the original B3 cartridge and the new prototype.

Using existing inventory at HAA, a sampling of mixers were tested using HAA's mixer test set and additional effort was put into improving the reliability of this test set. Four class A/B mixers were selected, measured, and installed within the existing B3 cartridge (see Fig. 9). Although the selection of mixers resulted in slightly higher-than-typical noise, it was decided to proceed so as not to delay the testing further.

Baseline testing of broadband SSB noise, narrowband SSB noise, and image-rejection were completed using our test cartridge. The cold part of the cartridge was rebuilt with the new DL-2SB prototype, as shown in Fig. 10. New support structures, brackets, and phase-matched cables were used, while the same mixers, IF stages (from the isolators back), and WCA were kept between the two versions. A comparison of the assembled cartridge and the prototype is shown in Fig. 10 (d). Note that in the original B3 cartridge, there are cold attenuators placed within the LO feeding waveguide; these attenuators were removed for the new cartridge configurations since the LO hole couplers are ~10 dB weaker coupling.

When comparing the baseline measurements with the prototype DL-2SB, there are several striking differences. Fig. 11 shows the measured broadband noise of (a) the original B3 cartridge and (b) the DL-2SB. In (a), the noise response follows a typical profile with the noise increasing at the RF signal band edges, whereas in (b), the profile is entirely different and appears to track the LO such that both the LSB and USB have similar profiles across varying LO frequency.

Despite this feature in the noise profile, there is a considerable reduction in noise—at some frequencies ~10 K—explained by the absence of the image termination and reduced RF signal loss through the LO coupler [3].

We performed a few measurement cycles to try to understand this behavior in the noise profile:

- Removing one polarization mixer pair and replacing them with waveguide loads
- Reversing the orientation of the mixer block and/or negatively biasing one mixer
- Swapping the WCA LO with an external Gunn oscillator
- Filtering the 2nd harmonic of the LO
- Removing all but one mixer to test in DSB mode

Fig. 12 shows the measured narrowband SSB noise where the same noise trends can be seen. However, an additional prominent ripple is observed across the IF response. Both the ripple and noise profiles track with the LO and are most serious at the low end, but improve at higher LO frequencies.

Finally, Fig. 13 shows the measured image rejection of the original B3 cartridge compared against the DL-2SB prototype. On average, the DL-2SB gave approximately 10 dB or better of image rejection, but it was originally hoped that the symmetry of the turnstile would improve image rejection further than this. We suspect that the same mechanism degrading the noise is also responsible for reduced sideband-separation, and further discussion is contained in Section 3.4.

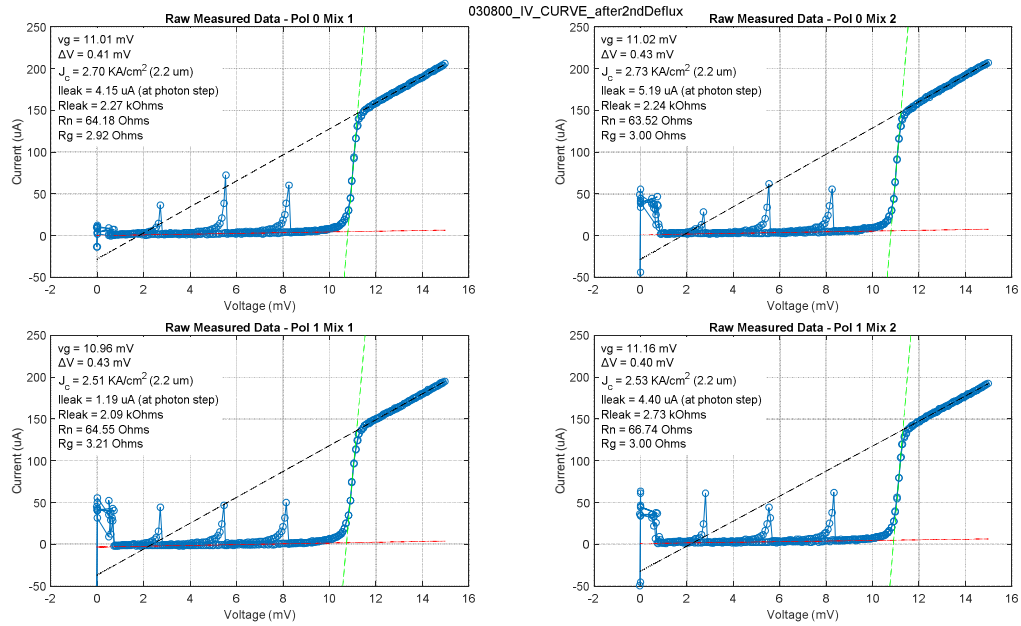


Fig. 9. DC characteristics of SIS mixers for comparison tests as measured in the cartridge test set (CTS). Pol 0 mixers have serial numbers 079 & 360 and pol 1 mixers have serial numbers 117 & 118.

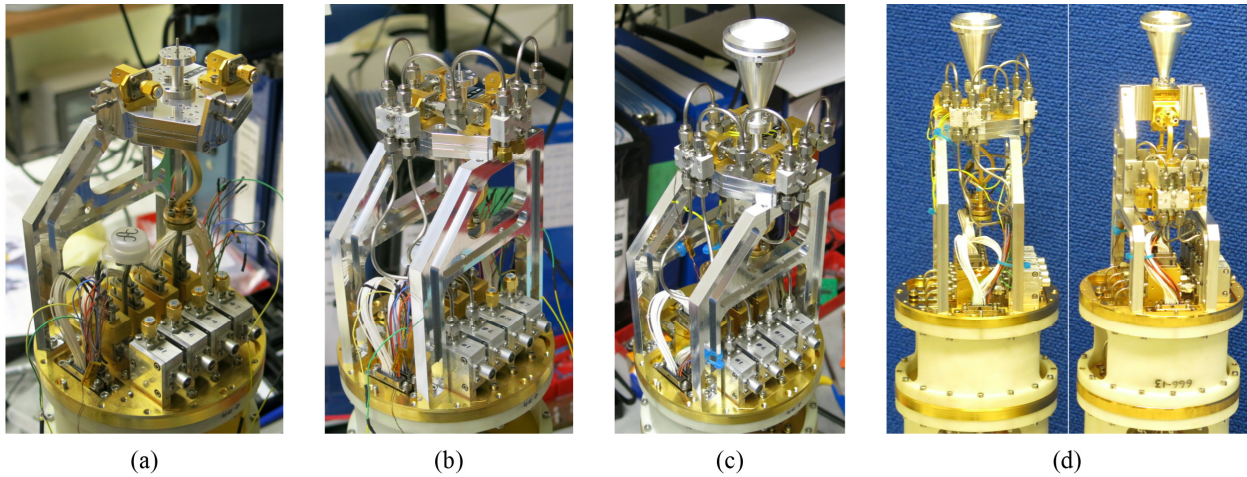
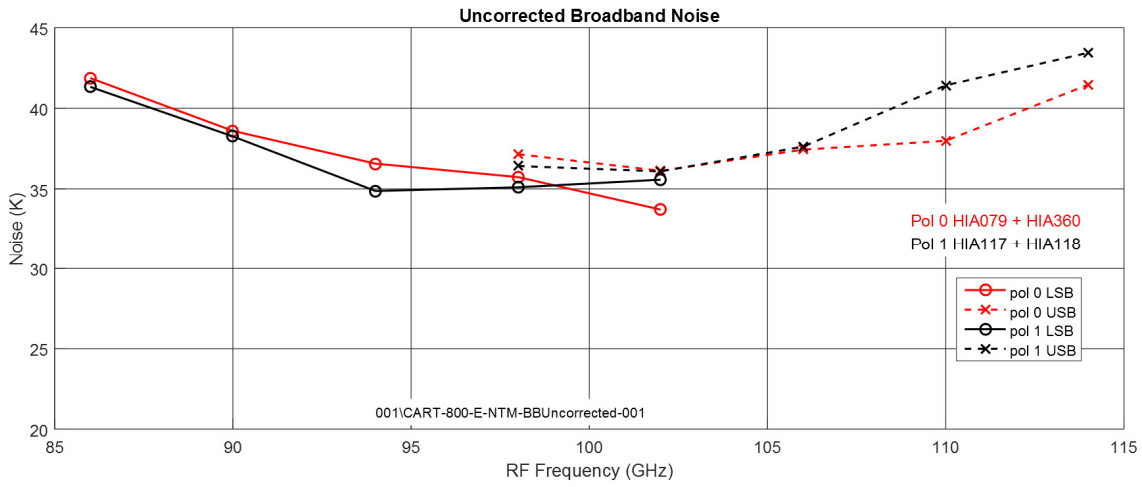
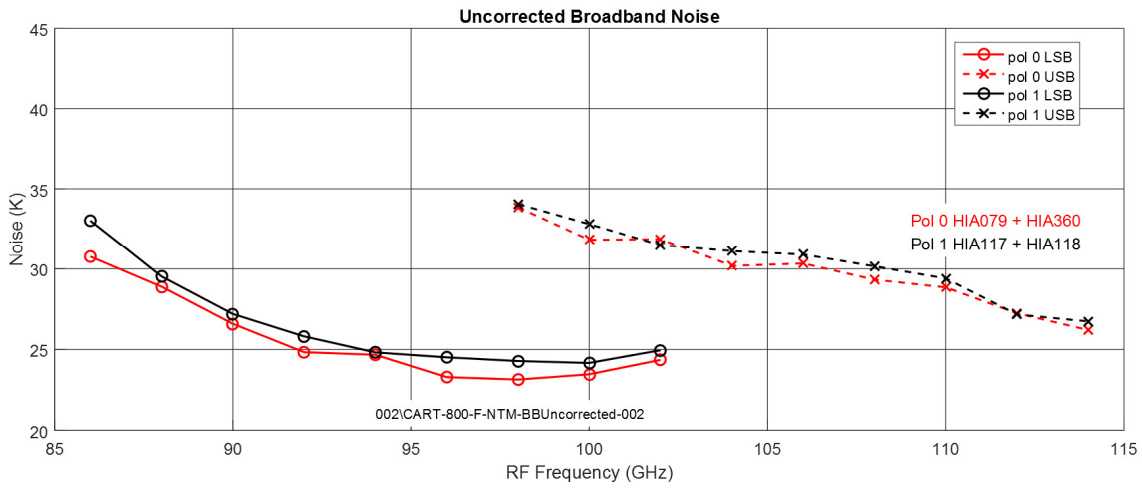


Fig. 10. Assembly pictures showing integration of the DL-2SB prototype into the B3 cartridge: (a) the DL-2SB connected to one LO output (the other is terminated), (b) the addition of the IF hybrids and phase-matched cables, and (c) the completed assembly. A side-by-side comparison of the cold stage between the original B3 cartridge and the prototype assembly is shown in (d).



(a)



(b)

Fig. 11. Measured broadband noise (i.e. within 4–8 GHz IF) for (a) the original B3 configuration and (b) the DL-2SB prototype.

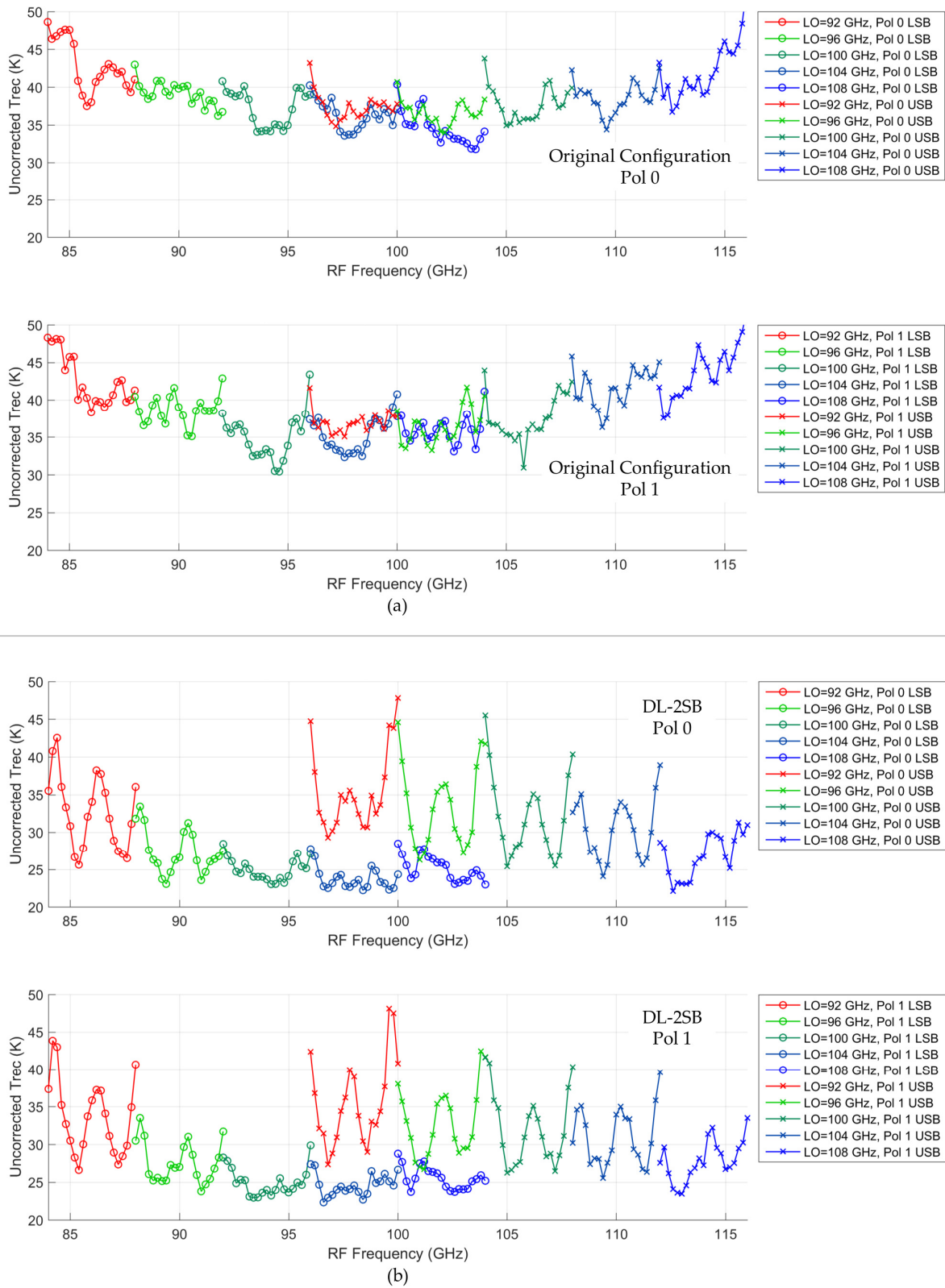


Fig. 12. Narrowband SSB noise comparison between (a) the original B3 cartridge configuration and (b) the DL-2SB prototype.

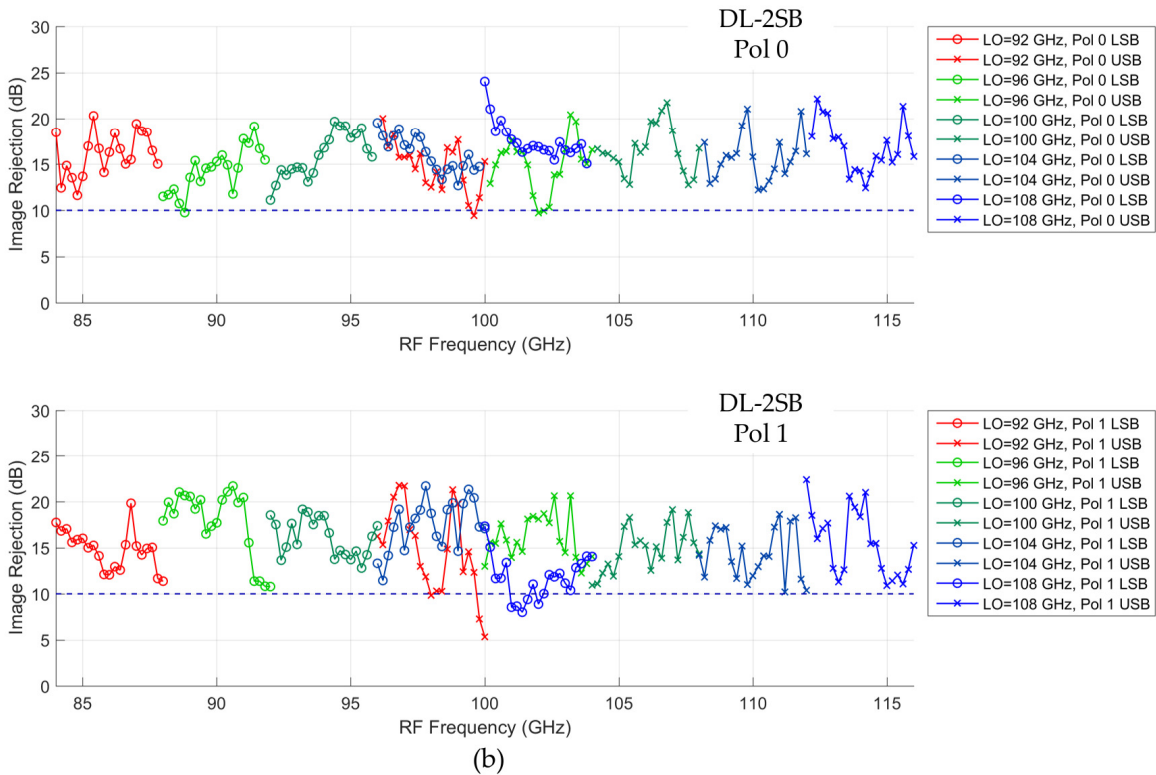
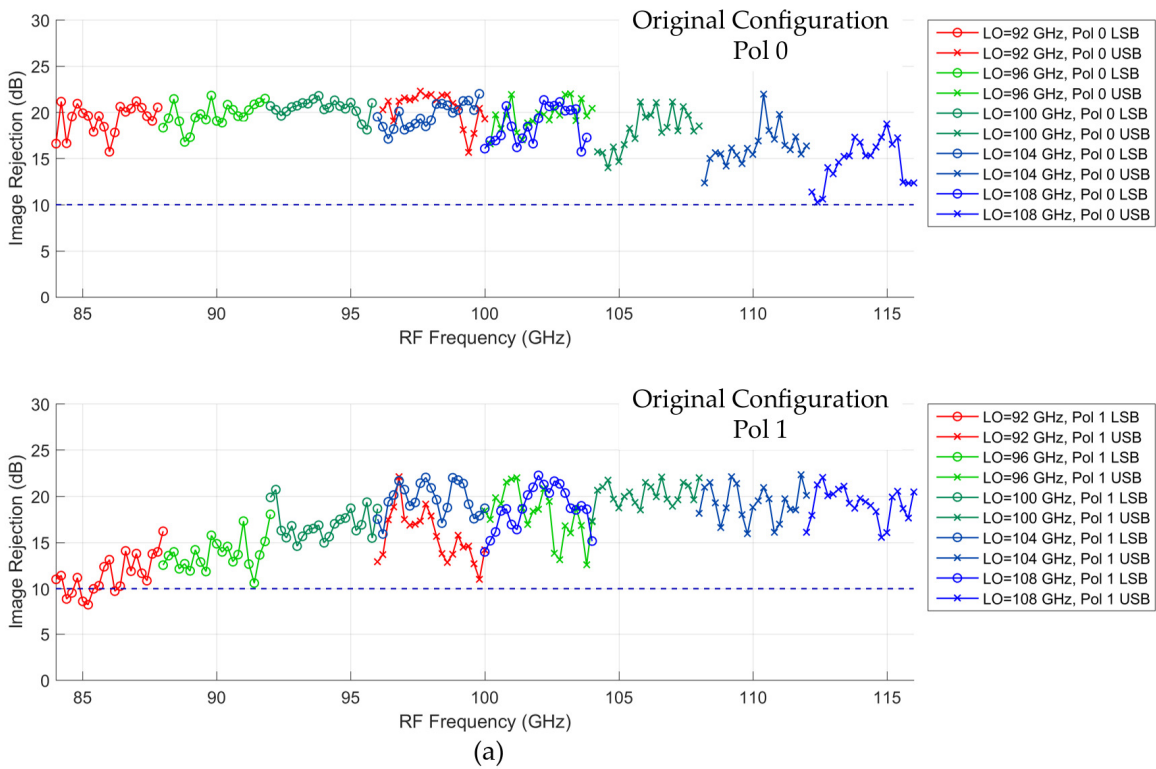


Fig. 13. Comparison of measured Image rejection between (a) the original B3 cartridge and (b) the DL-2SB prototype.

3 BAL-2SB

3.1 Design Overview

The second prototype (BAL-2SB) described in the study proposal is a single polarization, balanced, and sideband-separating block ([4], [7], [9]). The final design, shown in Fig. 14, is significantly different from the original proposal in order to simplify the layer stack-up and reduce the size. It is similar to that described in [4] and [9] except that the input RF is divided using the turnstile (therefore, there is no image termination).

Fig. 14 (a) and Fig. 15 illustrate that only one polarization is used from the turnstile and the other polarization is internally terminated with waveguide loads. The LO is divided in-phase using a 6-port hole coupler, followed by a pair of phase shifters acting on the upper and lower LO paths to pump each balanced mixer pair. Each balanced mixer pair is fed by a 3 dB hole coupler. Fig. 14 (b) shows the 4-pc machined assembly. The two middle layers have waveguides machined to a depth that leave a 0.006" thick wall from which the hole couplers are realized (initially, we had envisioned that the entire layer would be made from 0.006" shim stock, but in the end our machinist preferred to machine the thin wall directly).

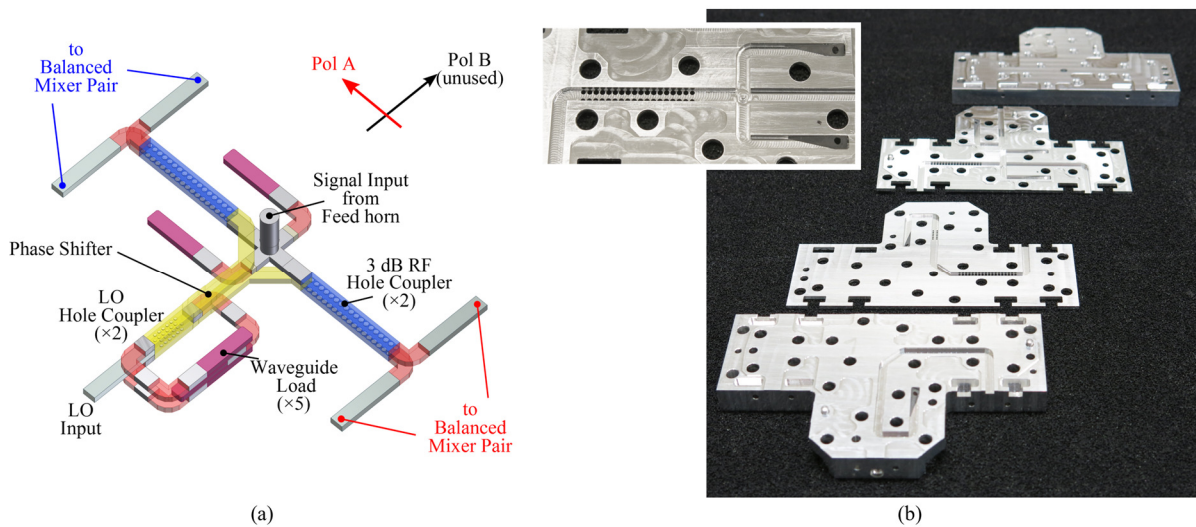


Fig. 14. Design concept for a balanced 2SB receiver (BAL-2SB). A CAD model of the waveguide channels is shown in (a) and the 4-layer machined block is shown in (b). A close-up of the turnstile and one of the 3 dB 90° hole couplers is shown inset.

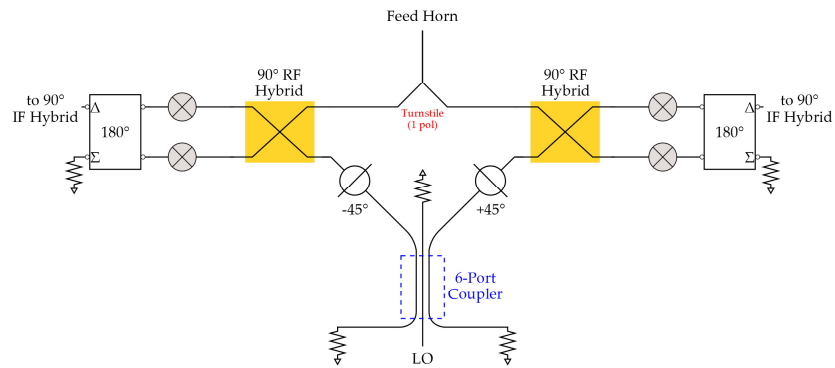


Fig. 15. Block diagram for balanced 2SB using a turnstile as input for one polarization.

A 6-port coupler, as shown in Fig. 16, was chosen to facilitate the platelet-type design such that the RF signal waveguides of the BAL-2SB block are along the same plane and membrane thicknesses are the same. For example, if a 4-port 3 dB coupler is used for the LO, the outputs would be on two separate, but adjacent, layers. From the turnstile, the split RF signal must be constrained to the same plane (or layer)—this means that the LO must either be on the same layer, or on a layer above and below the RF signal layer. Compared against a 3-port Y-splitter with phase shifters, a 6-port coupler is not loaded down by the phase shifters and all ports are matched which results in less ripple. The disadvantage of placing each coupler on a separate layer is that the couplers are fabricated under different machining set-up conditions which causes additional uncertainty.

See [10] and [11] for similar applications using 6-port hole couplers. As can be observed in Fig. 16 (b) and (c), the simulated input and output match is below -30 dB and the output isolation (S_{53}) is very high across the LO tuning range of 92–108 GHz. Assuming the ideal case that holes are identically defined, the amplitude imbalance is negligible and the phase balance is within a couple degrees.

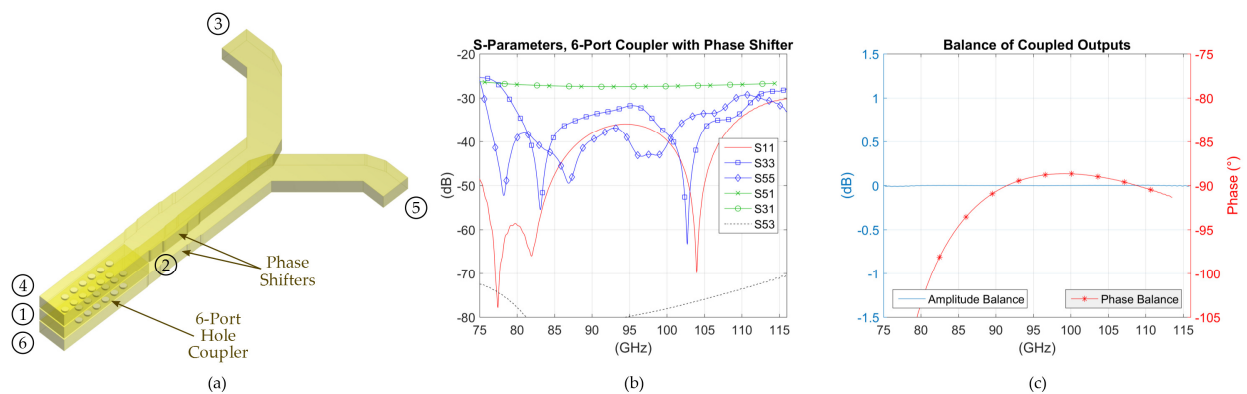


Fig. 16. (a) 6-port coupler with a pair of phase shifters on the coupled outputs. The simulated s-parameters of the coupler are shown in (b), indicating excellent port isolation (between ports 3 and 5) and good input reflection (S_{11} , S_{33} , and S_{55}). The phase and amplitude balance between S_{31} and S_{51} are shown in (c), demonstrating identical amplitude (assuming the ideal case that the holes are identical between layers) and smooth phase balance.

3.2 Measurements of the BAL-2SB Block

Measurements of the fully assembled BAL-2SB block are shown in Fig. 17. The results are divided into relevant s-parameters for the RF signal path, (a)–(d), and the LO path, (e)–(h). Port designations are shown inset: port 1 is the RF signal input (feed horn); ports 2–5 are the output mixer ports; and port 6 is the LO input.

The overall functioning of the balanced sideband-separating architecture depends on roughly twice as many components for proper overall balance. Balance is required for each output mixer pair (ports 2+3 and 4+5 in Fig. 17) but these pairs must be balanced with respect to each other. All four mixers should have similar gains, and IF recombination must be balanced through both the 180° and 90° IF hybrids.

Several comments may be made concerning the measured results of the BAL-2SB block. A general dissimilarity between the RF and LO results are the spikes within the RF path. As before, a circular-to-rectangular transition was used to inject a linearly polarized signal into port 1; since the circular port supports multiple modes and there is modal conversion around the turnstile region, these modes get trapped within the block. In practice, the circular port is terminated with a circular feed horn, so these modes are allowed to escape. Upon closer inspection in Fig. 17 (a)–(d), there are additional spikes around 100 GHz generated by a misalignment between block layers (simulation has shown that these trapped modes due to misalignment will also be allowed to escape when the circular port is terminated with the feed horn).

In looking at Fig. 17 (a) and (e), the input return loss for RF and LO ports is ~25 dB. The phase and amplitude differences of each balanced mixer pair are shown in (c), (d), (g), and (h). The mixer pair imbalance is essentially dictated by the 3 dB RF hole coupler, and is acceptable for decent balanced sideband-separation operation.

The mixer output return loss is also shown to be ~12–18 dB, indicating a 6 dB improvement compared to the DL-2SB case (attributed to the additional 90° 3 dB hole couplers). While the return loss and mixer-to-mixer isolation has improved in the BAL-2SB case, it is still not quite as good as one would first expect given that the RF hybrid alone has 40 dB isolation. As shown in Fig. 18, poor isolation is characteristic of both architectures and mixer-to-mixer isolation is limited to the value of the return loss. Even still, the BAL-2SB block has excellent LO isolation and should exhibit reduced ripple in the noise measurement because of the improved return loss and isolation.

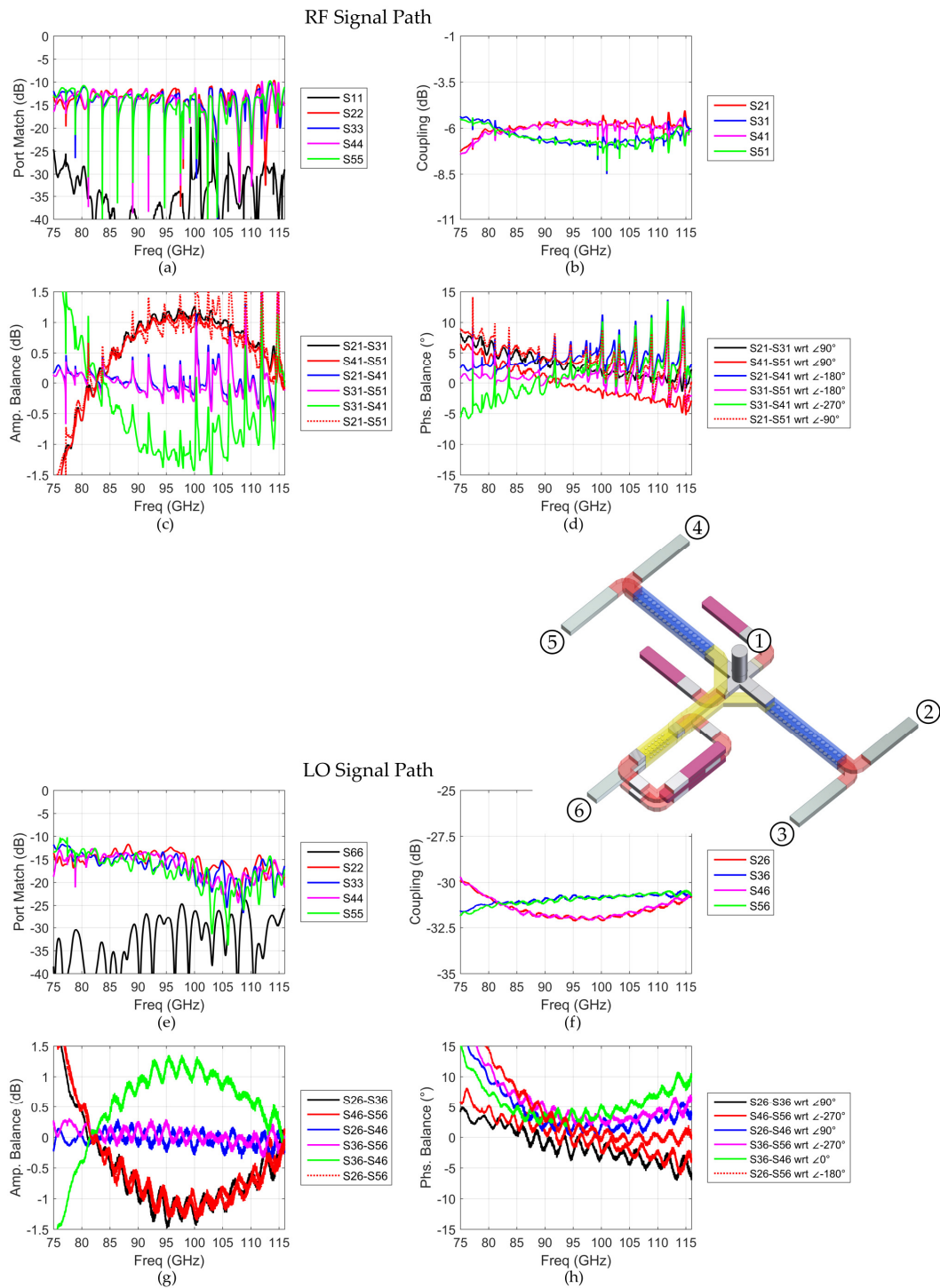


Fig. 17. Measured results of the BAL-2SB block. Note that port 1 is the input RF port, ports 2 & 3 and 4 & 5 are balanced mixer pairs, and port 6 is the LO input port (shown inset). (a)–(d) show the port reflection, coupling, and balance for the input RF signal path, while (e)–(h) show the responses for the LO path. The spikes shown in (a)–(d) result from a small misalignment between block layers and because port 1 was measured with a circular-to-rectangular transition. In (e)–(h), the spikes disappear because port 1 was left as an open-ended circular waveguide port allowing higher modes to escape.

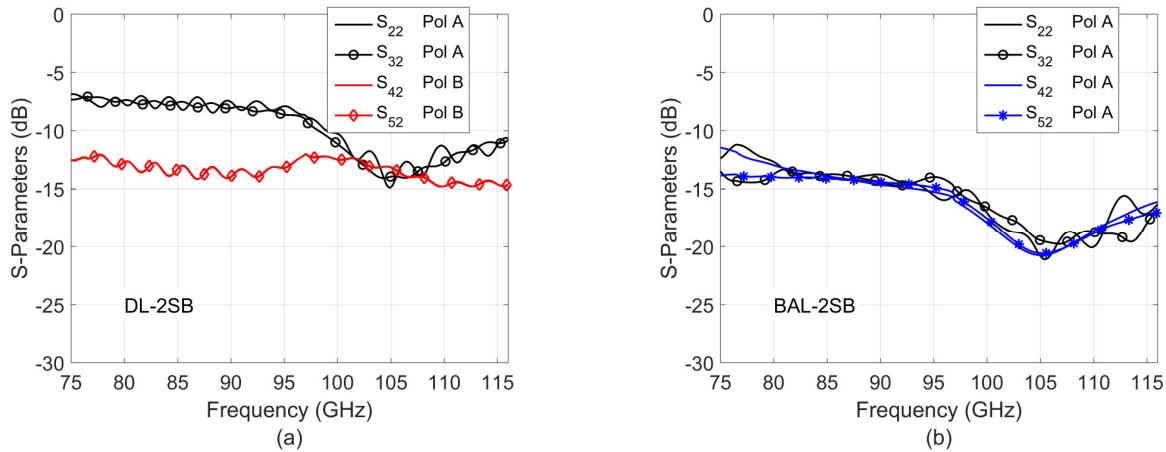


Fig. 18. Simulated s-parameters showing the relationship between mixer ports for the DL-2SB (a) and BAL-2SB (b) architectures. It is assumed that the input circular waveguide is terminated with a circular load or feed horn. In (a), S_{42} and S_{52} show leakage into the opposite polarization. Refer to Fig. 6 and Fig. 17 for port designations of each model. Note that mixer isolation within the same polarization is ~6 dB improved for the BAL-2SB model because of the additional 3 dB couplers.

3.3 Cartridge Integration

The balanced sideband-separating implementation requires additional 180° IF combiners and it is necessary for all four IF paths to be phase-matched. We used commercially available 4–12 GHz balanced couplers from KRYTAR (model 4040124) and found that we could achieve approximately 0.5 dB and 5° of balance when dipped in liquid nitrogen. The entire IF coupler and cable assembly, shown in Fig. 19, was measured to provide approximately 1 dB and 10° of balance at room temperature.

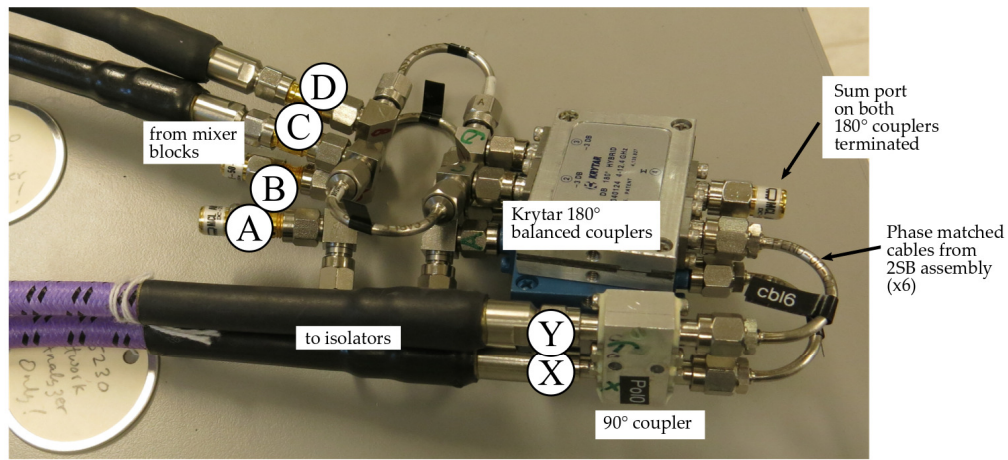
As is the case throughout this entire report, all mixer blocks are the same for each cartridge configuration, temperatures were held the same, and the same optics and IF stages were used.

Fig. 20 shows the full integration of the BAL-2SB block into an ALMA Band 3 receiver cartridge. Note that the emphasis of this configuration was on compatibility with the existing receiver cartridge, not overall compactness. In (a), the CAD model is shown for clarity where electrical mirror symmetry can be observed for each balanced mixer pair. The IF outputs of each balanced mixer pair are connected to the 180° balanced couplers. The diff port (Δ) of each 180° coupler are attached to the 90° hybrid for sideband-separation. Normally, the sum port (Σ) would be terminated by a cold 50Ω load and is where the LO sideband noise is terminated [9]. A complication arises, however, with the Band 3 cartridge because the SIS mixers are DC biased through a bias tee as part of each IF output. The BAL-DSB block is designed and oriented to only receive Pol 0, with two IF outputs (upper and lower sideband). Each of Pol 0 IF output is connected through a separate bias tee to provide DC bias for only one mixer. In the original ALMA B3 cartridge, the bias tee is contained within the LNA and the DC bias is routed through the center conductor and passes through the isolator and 90° hybrid. As such, in the BAL-2SB configuration, only two of the four mixers get biased through the IF outputs. We decided to attach the sum ports of each 180° coupler to the Pol 1 IF outputs to provide a reasonable termination and also allow the other two SIS mixers to be DC biased.

The BAL-2SB cartridge was cooled and Fig. 21 shows the measured receiver noise temperature and image-rejection in (a) and (b), respectively. Compared with Fig. 12, the BAL-2SB results do show an improvement in the noise ripple, especially in the lower sideband. The image rejection is quite

respectable, given the number of components required to be balanced, and is shown to be 10 dB (much of the band measured 15 dB or better). Fig. 21 (c) shows the measured noise comparison between the BAL-2SB configuration and the original Band 3 cartridge; the LSB shows a very clear improvement, while the USB has more ripple and once again shows an apparent LO-dependent response.

At the time of writing, there appear to be relatively few published measured results of balanced 2SB receivers for radio astronomy, but see [12] for an example. In Section 4.1, the final 90° IF combiner is removed to provide two balanced DSB outputs to compare against the balanced 2SB result. As a further note, an evanescent filter was machined to cut the 2nd harmonic of the LO; Fig. 22 shows its location within the cartridge. The filter was made to be 1 inch in length so that it could easily be replaced with a straight section of waveguide. After careful receiver noise measurements, we determined that there was an insignificant difference when the 2nd harmonic of the LO was filtered.



(a)

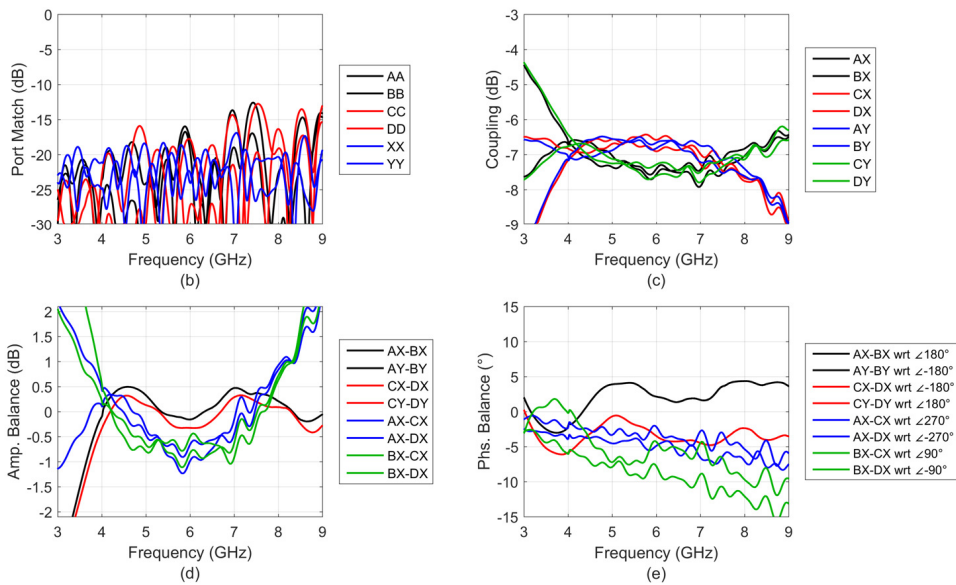


Fig. 19. Room temperature measurement of the IF coupler cable assembly that includes six phase-matched cables, eight right-angle adapters, two Krytar 180° balanced couplers, and one MAC 90° hybrid. Port designations are represented by the letters A, B, C, D, X, and Y.

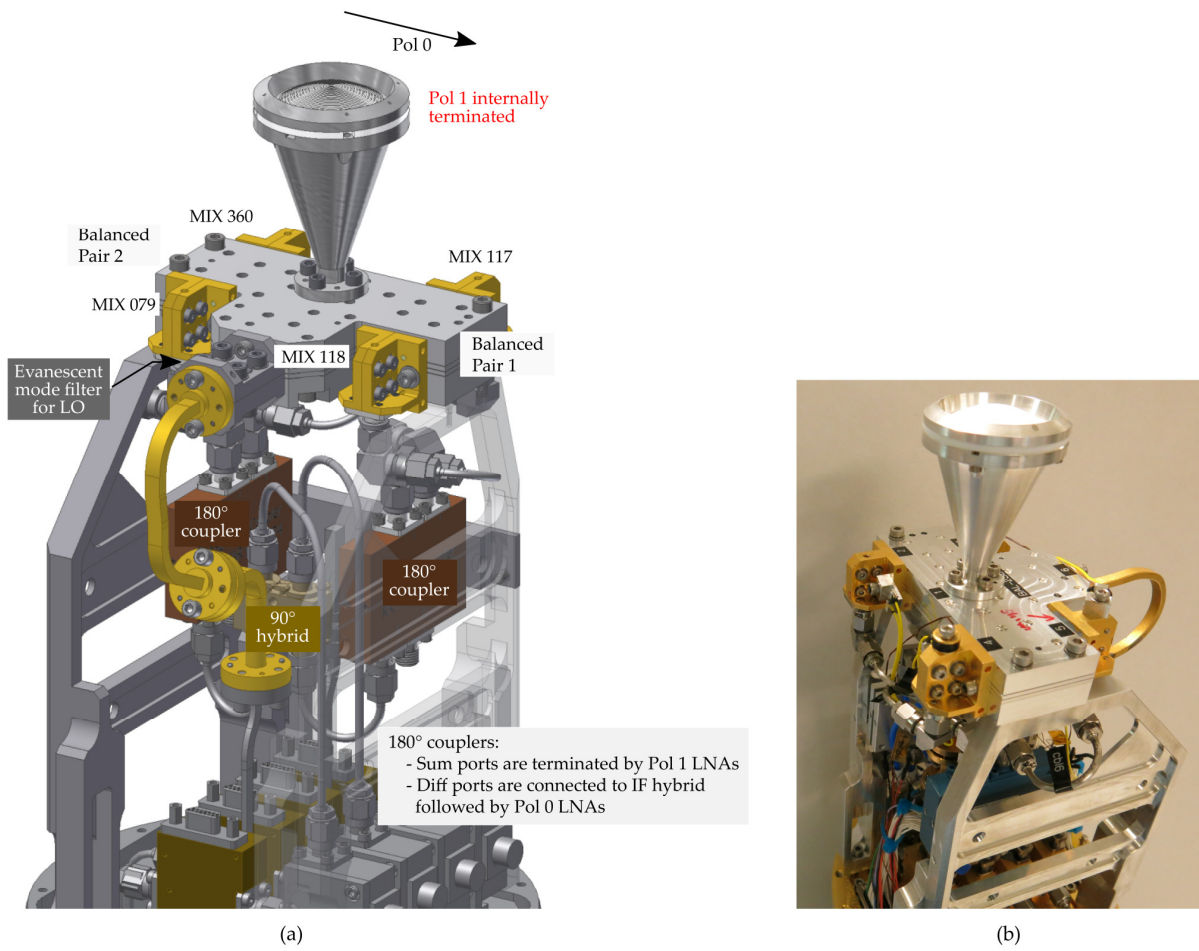


Fig. 20. (a) CAD view of the BAL-2SB cartridge assembly. All four mixer blocks are required for balanced sideband-separation of one polarization. Pol 1 is terminated using waveguide loads within the BAL-2SB block. (b) Realized BAL-2SB cartridge assembly.

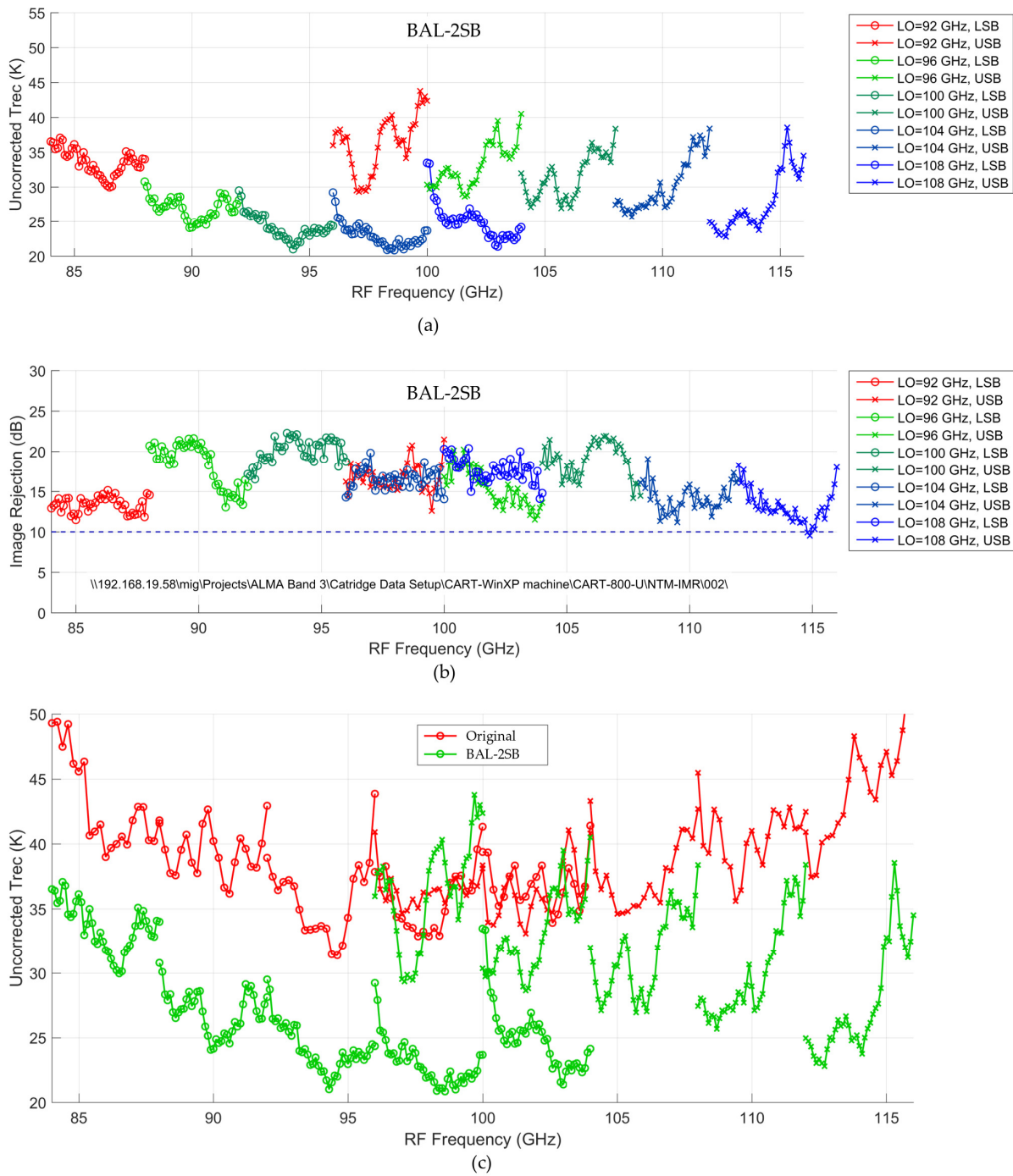


Fig. 21. Measured narrow-band receiver noise (a) and image-rejection (b) for the BAL-2SB cartridge configuration. In (c), the noise is compared with the original B3 cartridge.

3.4 A Closer Look at the Turnstile

In the proposal, we had incorrectly assumed that if the architecture was symmetric and balanced, then higher order modes would be rejected. It is indeed the case that if a TE_{11} mode is transduced (where TE_{11} is the desired linear polarization mode) and the block architecture is balanced and symmetric then only symmetric modes are excited with respect to the base exciting mode. It does not, however, preclude the situation where if another symmetric, balanced mode, such as TM_{01} or TE_{21} , is transduced within the feed horn, this mode will also be received through the turnstile, as illustrated in Fig. 22. To re-state this: there will be very little modal conversion from TE_{11} to TM_{01} and TE_{21} , but if the higher modes exist, they will propagate. As it turned out, simulation and block characterization with the VNA both used a linear excitation (VNA measurements used a circular to rectangular transition). Furthermore, when the sideband interference measurement was conducted, the sideband interferer was injected towards the cartridge window using an open-ended rectangular waveguide that also induced a TE_{11} mode. The base conditions are different, however, when the noise temperature was measured using black-body calibration loads; here the polarization from each black-body load is random and energy may be transduced within the circular guide in any of the higher order modes that are supported. This can give rise to the situation where the image-rejection appears fine from measurement, yet receiver noise measurements have degraded.

As shown in Fig. 22, the TM_{01} and TE_{21} modes are perfectly balanced when divided by the turnstile; the key difference with respect to the fundamental TE_{11} mode is that the branch outputs are in-phase (in contrast to the divided outputs of the TE_{11} mode that have 180° difference). Fig. 23 shows the simulation of the DL-2SB block when modes 1(3) and 1(4), TM_{01} and TE_{21} respectively, excite the block. Although the port reflection is not good for these modes, there is noticeable transmission; this does not show how much energy is transduced from a randomly-polarized black-body, but rather how that specific field configuration would propagate if present. Due to the cut-off, the TE_{21} mode is only present in the upper half of the band. In Fig. 23 (d) and (e), one can see how since the phase propagation constant and weighting coefficient is different for each higher mode, their contribution will cause ripple in the gain and overall balance of block outputs. In fact, since the TM_{01} and TE_{21} modes have in-phase power division through the turnstile, it is akin to introducing a phase-reversal within one branch of the 2SB architecture that effectively swaps the IF outputs between LSB and USB. As such, the “LO-dependent response” observed in the noise measurements may be understood as an imbalance resulting in a DSB imprint onto the measured noise response. Of course, these modes are also detrimental with regard to cross-polarization.

The turnstile works well within a symmetric OMT because the output branches are combined with an E-plane Y-combiner (i.e., a 3-port 180° combiner), and in-phase power within the branches from higher order modes are reflected (see example in Fig. 24). Another method is shown in [13]–[15], where a planar OMT is used and branch outputs are combined through a 4-port balanced coupler such that the higher order modes are terminated.

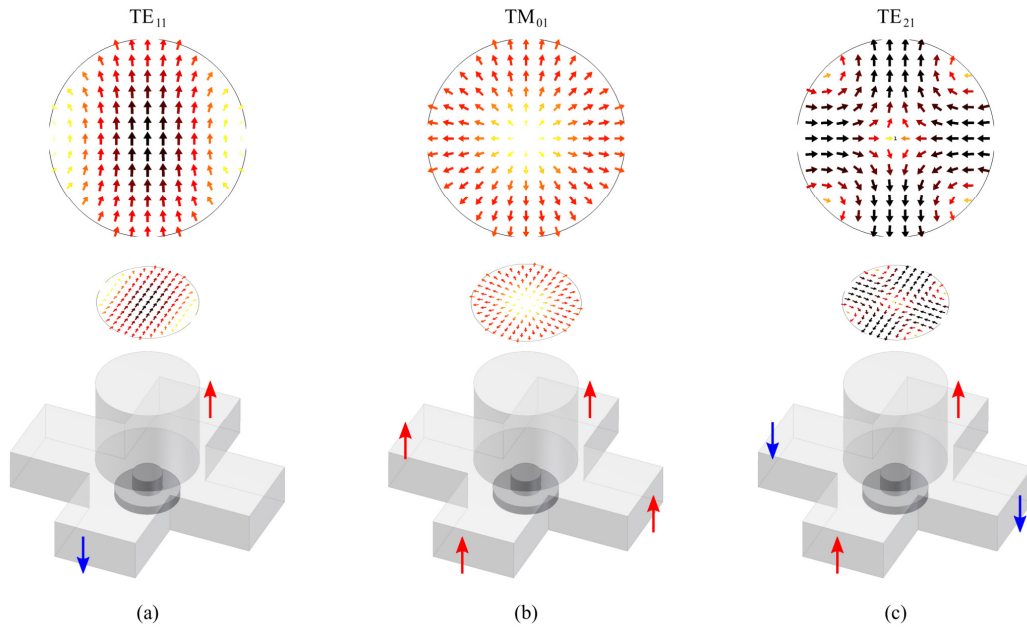


Fig. 22. Balanced and symmetric modes that may be transduced by the circular guide and turnstile.

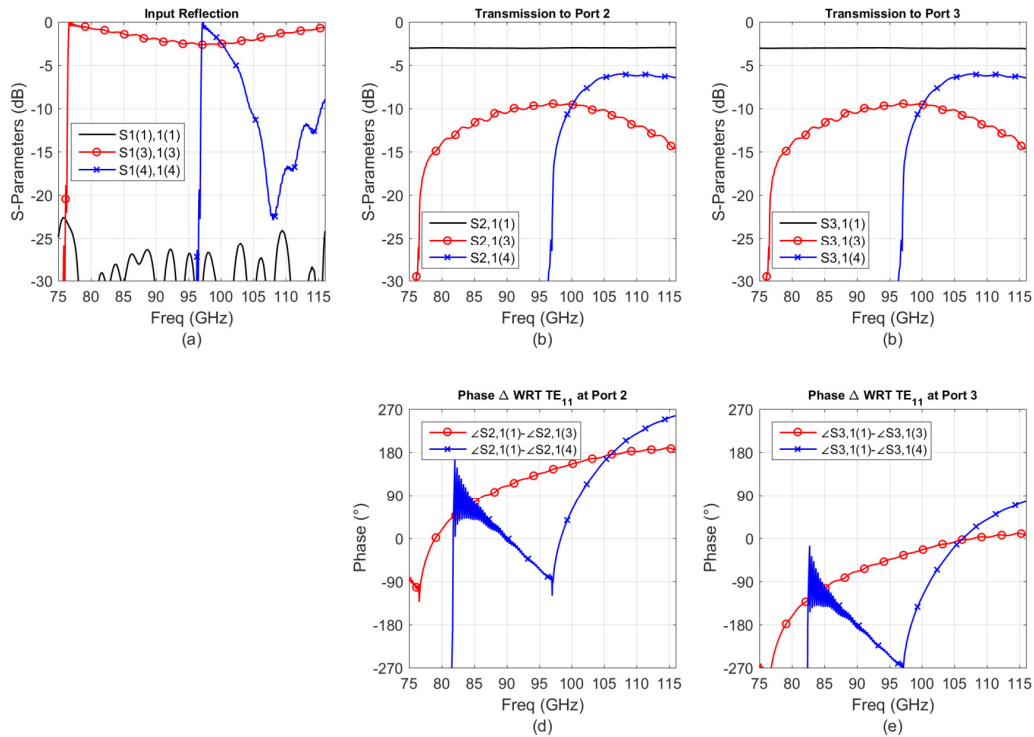


Fig. 23. Simulated propagation of balanced modes for the DL-2SB block model. Modes 1(1), 1(3), and 1(4) refer to TE_{11} , TM_{01} , and TE_{21} , respectively.

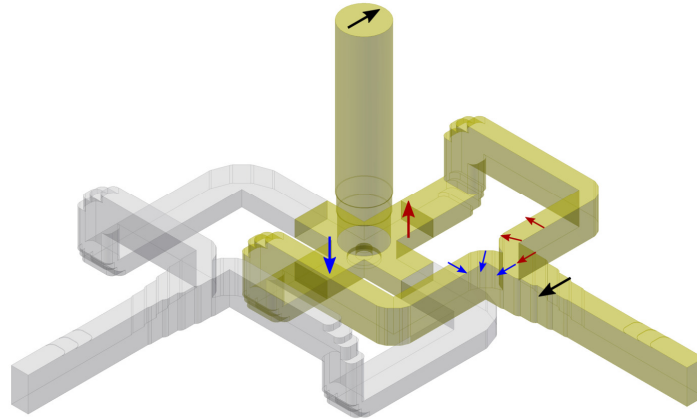


Fig. 24. Example usage of an E-plane combiner showing recombination assuming an aligned TE_{11} excitation; in this case, TM_{01} and TE_{21} modes are shorted out.

4 Supplementary Experiments

In addition to the baseline testing, we conducted many additional tests, with the two most relevant results included here.

At the end of the study period, the test cartridge was reconfigured to its original B3 design and reference measurements were taken that showed consistency with those measurements taken at the beginning of the study over one year prior.

4.1 BAL-DSB: Removing the 90° IF Hybrid

Considering the 2nd prototype architecture, the BAL-2SB receiver can be made into two balanced DSB outputs by simply removing the final 90° IF hybrid (See Fig. 15 for reference). In this case, there will be two balanced DSB outputs, and since the signal gain has been split in half, the DSB results are comparable to the 2SB noise measurements (given there is sufficient image rejection).

Fig. 25 shows the measured receiver noise plotted with respect to the LO frequency for: (a) the balanced sideband-separated configuration and (b) when the 90° IF hybrid is removed to give two balanced double-sideband outputs. In (b), the ripple has improved. If we assume that higher modes are present within the turnstile, the balanced DSB outputs do not suffer in the same way because energy received through each mode undergoes the same phase through the balanced section—it is only when the powers are finally recombined from each half of the turnstile output that the phases interfere. Also, since the sum ports (Σ) of the balanced IF couplers were connected to LNAs instead of a simple termination, we were able to confirm that the balanced architecture (i.e., the signal recombining at the Δ -port) was indeed providing proper signal isolation between the balanced IF coupler outputs (roughly 15 dB).

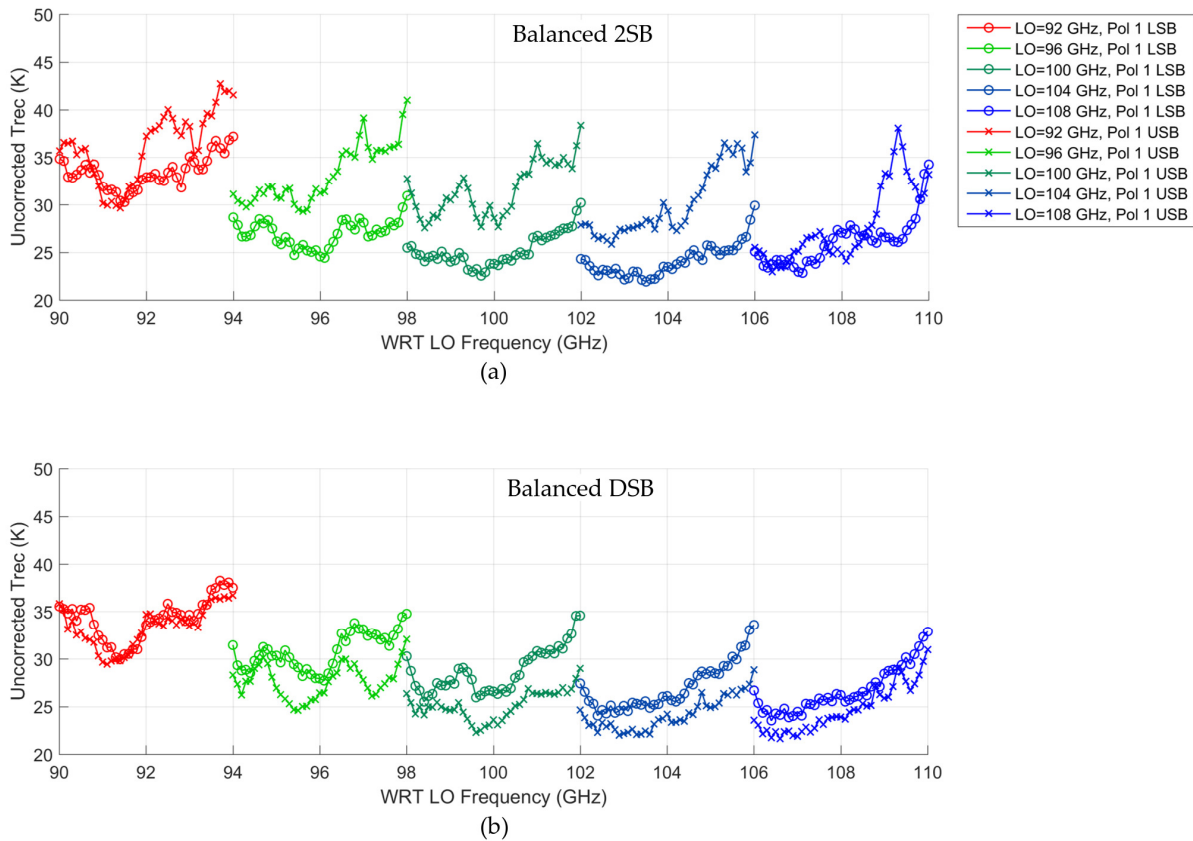


Fig. 25. Measurement comparison of the 2nd prototype in: (a) its full balanced sideband-separated configuration and (b) when the 90° IF hybrid is removed to provide two balanced double-sideband output signals. In (a), the outputs correspond to LSB and USB, but in (b), each output is DSB measured through the corresponding IF chain. In (b), it is important to remember that the RF signal has been split in half; as such, these DSB results are more comparable with SSB receiver noise.

4.2 Reversing LO/RF Inputs on the B3 Cartridge

Given the lack of isolation within the turnstile (similar to a 3-port power splitter), and also the discussion around possible higher modes within the circular guide, an appropriate test is to simply switch around the inputs of the hybrid block within the nominal B3 2SB assembly.

The ALMA B3 mixer block includes a parallel waveguide channel to house the termination for the LO path and, in order to flip the RF and LO inputs on the hybrid block, an adapter plate was designed to offset the mixer block. Fig. 26 (a) shows the cut-away detail of the hybrid block when used with the new adapter. In (b), the adapter plates have been installed into the cartridge only within the Pol 0 path so that the Pol 1 path can serve as a reference.

By replacing the 4-port branch-line coupler along the RF path with a 3-port Y-splitter, we should see a drop in noise (since the image termination has been removed) at the expense of higher ripple due to standing waves between the mixer block and Y-junction. One interesting consequence to using the 90° branch-line coupler for the LO is that the pumping amplitude between mixers is more uneven depending on the LO frequency.

Fig. 27 shows the comparison of narrow-band noise when the hybrid block is flipped. The standing wave between the Y-junction and each mixer block is apparent, and essentially demonstrates that the mixer pair does not work in concert to cancel these reflections. Furthermore, we do not observe the “LO dependent” response which corroborates that this response was due to higher modes within the circular guide and turnstile (see Section 3.4). Here, the ripple is much more pronounced, as compared to the prototypes above, despite the appearance of relatively good image-rejection shown in (c).

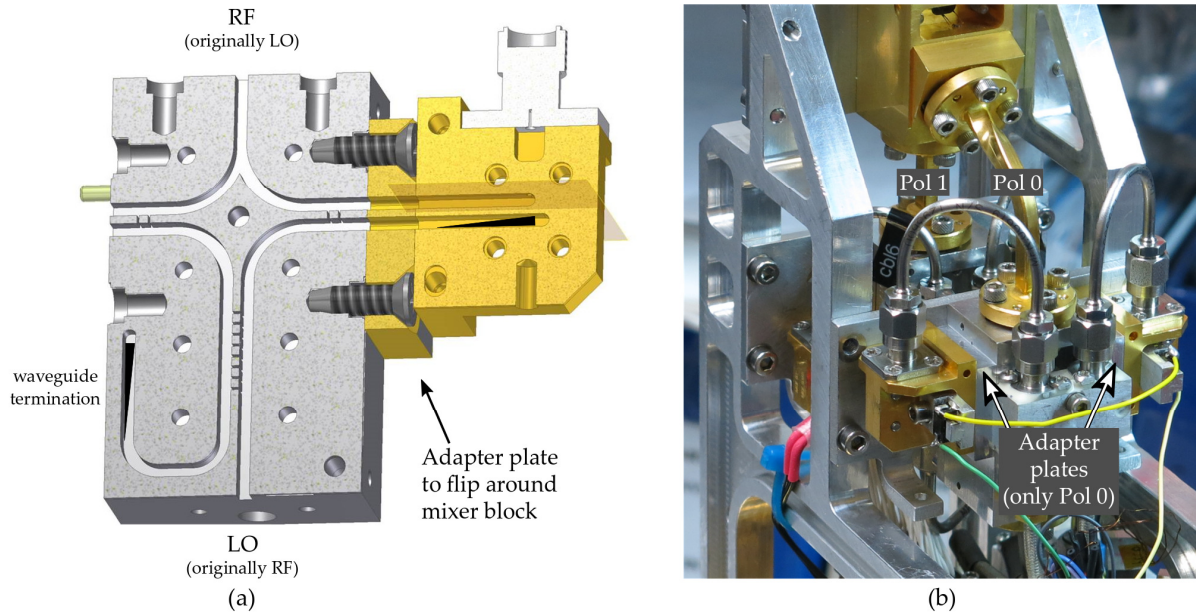


Fig. 26. (a) Illustration showing how the RF/LO input was flipped by means of an adapter plate between the mixer block and the hybrid block. Only one side is shown for clarity, but both adapter plates were machined to the same thickness to preserve phase balance. The LO is still coupled into the RF path by ~16 dB couplers. Since the RF is now split through the Y-splitter, the outputs are no longer isolated. The fourth port waveguide termination has also been moved to the LO side and no longer contributes 4 K noise into the RF path. Only one polarization within the B3 cartridge was modified, as shown in (b).

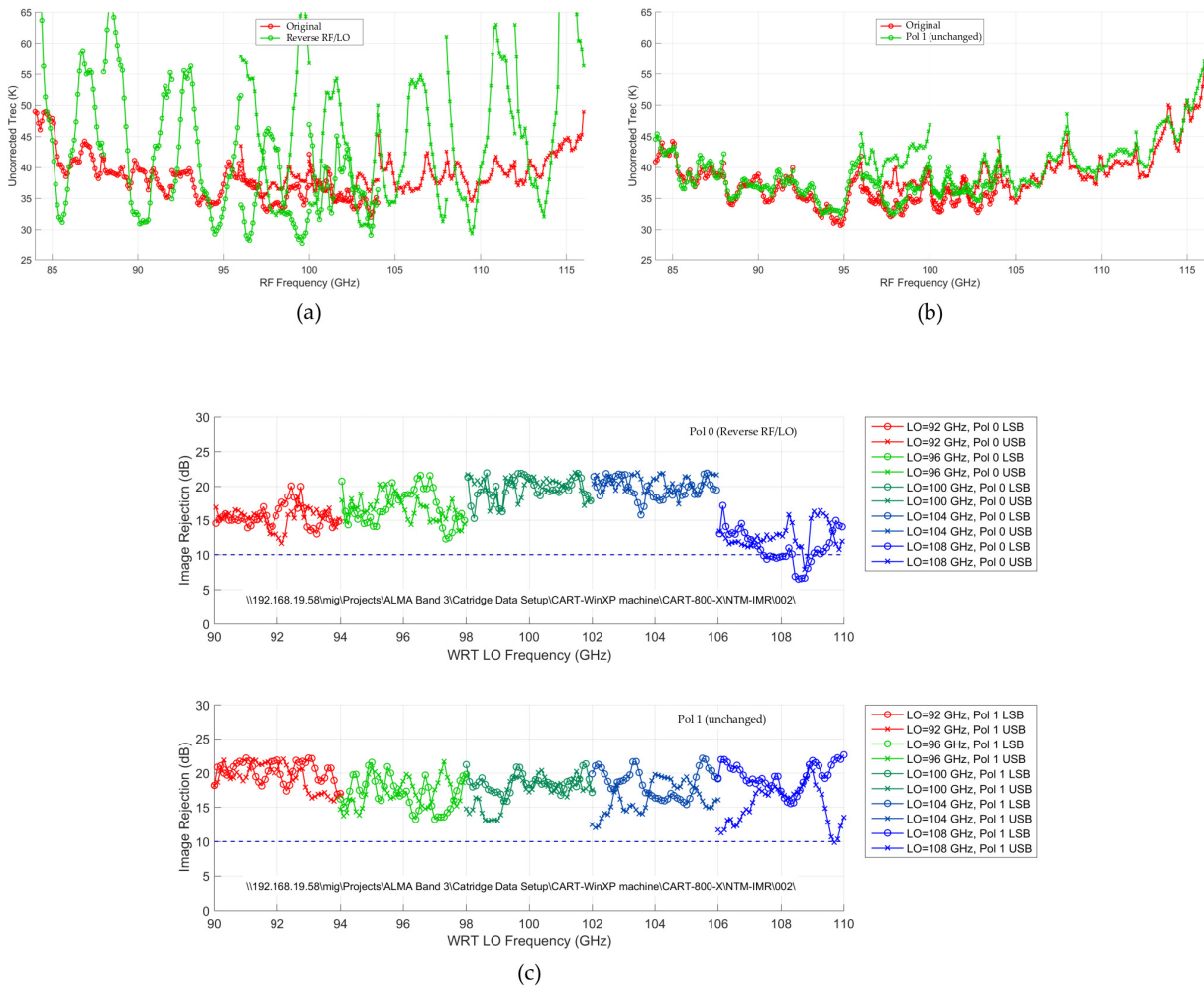


Fig. 27. Narrowband noise measurements comparing the effect of swapping the RF/LO inputs. (a) Pol 0 shows the case where the hybrid block has been flipped upside-down so that the RF signal is injected through the y-splitter (green curve). The results are plotted together with a reference measurement (red curve) of the cartridge in its baseline configuration. (b) Pol 1 was not modified. (c) With the exception of LO=108 GHz, the image rejection remained quite good, indicating that overall balance was maintained during the port reversal.

5 Conclusion and Future Outlook

One of the primary goals of the study was to explore a platelet-style architecture that could be applicable to arrays of dual-linear sideband-separating receivers, namely for LO distribution and OMT integration.

In the DL-2SB design, the RF path and LO paths were contained along the same layer, such that for arrays, the distribution of RF and LO were machined into a single piece with relative machine precision for the entire distribution path. This technique was successful, as all four mixers were evenly pumped using the same LO feed and very similar responses were observed for both polarizations. The LO output (i.e., the signal remaining after pumping the mixers) remained balanced and suitable to continue pumping more mixers. The platelet structure was also conducive to broad-wall hole couplers, which were shown to be quite machinable, and reproducible, for the given low values of coupling (\sim -30 dB), and could be well-suited towards other planar processing techniques.

Integrating the turnstile as an OMT/power divider for sideband-separation was shown to be problematic. The mixer pairs did not appear to be balanced enough to reduce standing waves at the mixer input, and, balanced higher order modes within the circular waveguide and turnstile degraded the noise and image rejection measurement.

The BAL-2SB design showed similar success with the LO distribution, and overall good balance was achieved throughout the RF, LO, and IF paths, as demonstrated by the measured image rejection. Ripple in the noise was reduced, but a similar degradation in noise due to the turnstile was observed.

In Fig. 28, a design concept is shown that adapts the positive outcomes of this study. In particular, magic-T 180° couplers are used to increase isolation and output match to reduce the interaction between mixers (similar to that shown in [16]). The RF signal inputs are assumed to be collinear so that it is easy to route and reuse the LO pumping signal. All hole couplers are defined within the same layer for repeatability in manufacturing and the block may be separately characterized for verification. Since the baseline design of the B3 cartridge has collinear outputs from the OMT, the concept may be tested within the cartridge, as shown in Fig. 28 (b).

As a final note, for the comparative measurements presented herein, we found it extremely beneficial to make use of the ALMA B3 cartridge, test set, and individual mixer blocks to help control the testing environment.

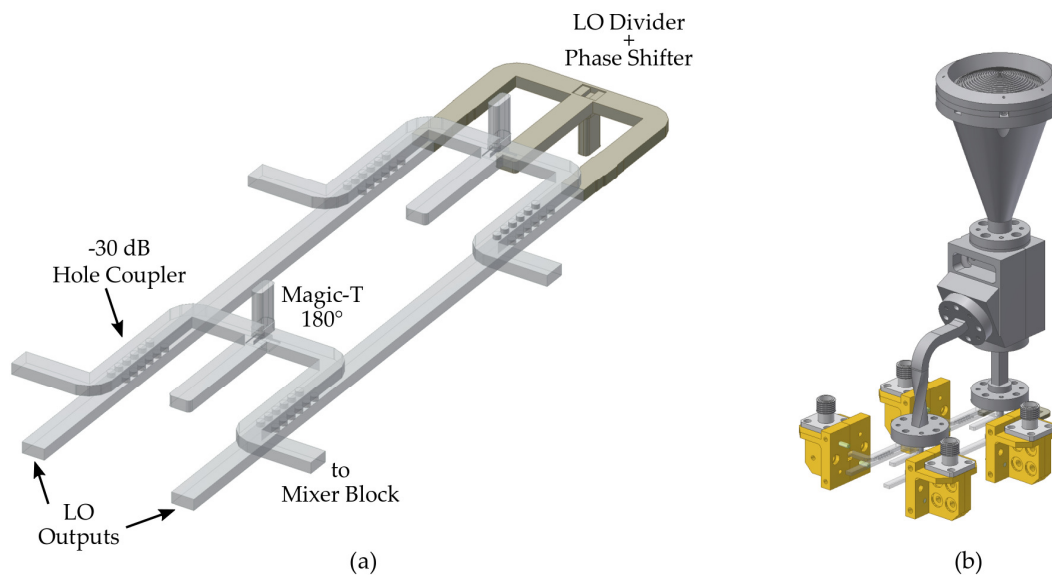


Fig. 28. (a) Concept for future implementation of a sideband-separating network showing how the LO is distributed using broad-wall hole couplers. The RF signal is divided using a magic-T for added mixer-to-mixer isolation and multiple 2SB assemblies may be cascaded if the RF outputs from each OMT are in-line. The concept may be adapted to incorporate the original B3 OMT as shown in (b).

Acknowledgments

In addition to the co-investigators listed in Section 1.1, the following invaluable contributions are acknowledged: Felipe Miranda for contributions to the manufacturability of the design and exceptional machining; Neal Kelly for precise machining of the evanescent-mode filter and adapter plate; Ivan Wevers for completing the mechanical design of each block and overcoming the design challenges of cartridge integration; and Corinne Rai for careful project management. Thanks to Mike Romero of KRYTAR, inc., who provided us with additional 180° couplers for cryogenic testing.

Appendix A - Reference Documents

- [1] D. Henke, P. Niranjana, and L. Knee, "Prototype of a Complete Dual-Linear 2SB Block and a Single-Polarization Balanced 2SB Block," Cycle 4 ALMA Development Study Proposal, May, 2016.
- [2] D. Henke, "Interim Report, January 2018: Prototype of a Complete Dual-Linear 2SB...", NRC Herzberg, Victoria, Canada, Jan. 30, 2018.
- [3] A. R. Kerr, S.-K. Pan, S. M. X. Claude, P. Dindo, A. W. Lichtenberger, J. E. Effland, and E. F. Lauria, "Development of the ALMA Band-3 and Band-6 Sideband-Separating SIS Mixers," *IEEE Trans. THz Sci. Technol.*, vol. 4, no. 2, pp. 201–212, Mar. 2014.
- [4] S. Claude, C. Cunningham, A. R. Kerr, and S.-K. Pan, "Design of a Sideband-Separating Balanced SIS Mixer Based on Waveguide Hybrids," ALMA Memo 316, Sept. 2000. [Online]. Available: <http://library.nrao.edu/alma.shtml>.

- [5] J. Dittloff, F. Arndt, and D. Grauerholz, "Optimum design of waveguide E-plane stub-loaded phase shifters," *IEEE Trans. Microw. Theory Tech.*, vol. 36, no. 3, pp. 582–587, Mar. 1988.
- [6] D. Henke, I. Wevers, P. Niranjana, and L. Knee, "2SB and Balanced Receiver Architectures using Hole Couplers," in *URSI GASS*, Montreal, QC, pp. 1-3, Aug. 19–26, 2017.
- [7] A. R. Kerr and S.-K. Pan, "Design of planar image-separating and balanced SIS mixers," in *Proc. 7th Int. Symp. Space Terahertz Technol.*, Mar. 12–14, 1996, pp. 207–219.
- [8] A. R. Kerr, S.-K. Pan, E. F. Lauria, A. W. Lichtenberger, J. Zhang, M. W. Pospieszalski, N. Horner, G. A. Ediss, J. E. Effland, and R. L. Groves, "The ALMA Band 6 (211-275 GHz) Sideband-Separating SIS Mixer-Preamplifier," in *Proc. 15th Int. Symp. Space Terahertz Technol.*, Apr. 27–29, 2004, pp. 55–61.
- [9] A. R. Kerr, J. Effland, A. W. Lichtenberger, and J. Mangum, "Towards a Second Generation SIS Receiver for ALMA Band 6," NRAO, Charlottesville, VA, Mar. 23, 2016.
- [10] N. Erickson, "High Performance Dual Directional Couplers for Near-mm Wavelengths," *IEEE Microw. Wireless Comp. Lett.*, vol. 11, no. 5, pp. 205–207, May 2001.
- [11] E. W. Bryerton, "A Cryogenic Integrated Noise Calibration and Coupler Module Using a MMIC LNA," *IEEE Trans. Microw. Theory Tech.*, vol. 59, no. 8, pp. 2117–2122, Aug. 2011.
- [12] Y. Serizawa et al., "Development of a 385–500 GHz sideband-separating balanced SIS mixer," *J. Infrared, Millimeter THz Waves*, vol. 33, pp. 999–1017, 2012.
- [13] G. Engargiola and R. L. Plambeck, "Tests of a planar L-band orthomode transducer in circular waveguide," *Review of Scientific Instruments*, vol. 74, no. 3, pp. 1380–1382, 2003.
- [14] S. Shu et al., "Development of octave-band planar ortho-mode transducer with kinetic inductance detector for LiteBIRD," *Proc. SPIE*, vol. 9914, pp. 1–6, 2016.
- [15] W. Shan et al., "A new concept for quasi-planar integration of superconductor-insulator-superconductor array receiver front ends," *IEEE Trans. THz Sci. Technol.*, vol. 8, no. 4, pp. 472–474, Jun. 2018.
- [16] R. L. Akeson, J. E. Carlstrom, D. P. Woody, J. Kawamura, A. R. Kerr, S.-K. Pan, and K. Wan, "Development of a sideband separation receiver at 100 GHz," in *Proc. 4th Int. Symp. Space Terahertz Technol.*, pp. 12-17, March 1993.